Volume III

Midwestern Regional Carbon Sequestration Partnership (MRCSP) Phase III (Development Phase)

Cross-Well Seismic Monitoring of CO_2 Injected Into the A-1 Carbonate and Brown Niagaran Formations at the Chester 16 Reef

Prepared by:

Battelle
505 King Avenue
Columbus, Ohio 43201

Principal Investigator: Dr. Neeraj Gupta

Authors: Mark Kelley, Conrad Kolb, and Neeraj Gupta

Submitted to:

The U.S. Department of Energy, National Energy Technology Laboratory
Program Manager: Andrea McNemar

DOE MRCSP Project #DE-FC26-05NT42589

September 2020

BATTELLE

Notice

This report was prepared by Battelle as an account of work sponsored by an agency of the United States Government and other project sponsors, including Core Energy, LLC and The Ohio Development Services Agency. Neither the United States Government, nor any agency thereof, nor any of their employees, nor Battelle and other cosponsors, makes any warranty, express or implied, or assumes any liability or responsibility for the accuracy, completeness, or usefulness of any information, apparatus, product, or process disclosed, or represents that its use would not infringe privately owned rights. Reference herein to any specific commercial product, process, or service by trade name, trademark, manufacturer, or otherwise does not necessarily constitute or imply its endorsement, recommendations, or favoring by the United States Government or any agency thereof. The views and the opinions of authors expressed herein do not necessarily state or reflect those of the United States Government or any agency thereof.

Battelle does not engage in research for advertising, sales promotion, or endorsement of our clients' interests including raising investment capital or recommending investments decisions, or other publicity purposes, or for any use in litigation.

Battelle endeavors at all times to produce work of the highest quality, consistent with our contract commitments. However, because of the research and/or experimental nature of this work the client undertakes the sole responsibility for the consequence of any use or misuse of, or inability to use, any information, apparatus, process or result obtained from Battelle, and Battelle, its employees, officers, or Trustees have no legal liability for the accuracy, adequacy, or efficacy thereof.

Acknowledgements

Sponsorships - This report is part of a series of reports prepared under the Midwestern Regional Carbon Sequestration Partnership (MRCSP) Phase III (Development Phase). These reports summarize and detail the findings of the work conducted under the Phase III project. The primary funding for the MRCSP program is from the US Department of Energy's National Energy Technology Laboratory (NETL) under DOE project number DE-FC26-05NT42589 with Ms. Andrea McNemar as the DOE project manager. The past DOE project managers for MRCSP include Dawn Deel, Lynn Brickett, and Traci Rodosta. Many others in the DOE leadership supported, encouraged, and enabled the MRCSP work including but not limited to Kanwal Mahajan, John Litynski, Darin Damiani, and Sean Plasynski.

The Michigan Basin large-scale test received significant in-kind cost share from Core Energy, LLC, who also provided essential access to the field test site and related data. This contribution by Core Energy CEO Robert Mannes, VP Operations Rick Pardini, and Allan Modroo, VP Exploration, and the entire Core Energy staff is gratefully acknowledged. MRCSP work in Ohio has been supported by the Ohio Coal Development Office in the Ohio Development Services Agency under various grants (CDO D-10-7, CDO-D-13-22, CDO-D-D-13-24, and CDO-D-15-08) with Mr. Greg Payne as the OCDO project manager. Finally, several industry sponsors and numerous technical team members from State Geological Surveys, universities, and field service providers have supported MRCSP through cash and in-kind contributions over the years as listed in the individual reports.

Program Leadership – During the MRCSP Phase III project period, several Battelle staff and external collaborators contributed to the successful completion of the program through their efforts in field work, geological data analysis and interpretation, and/or reporting. The primary project managers over the MRCSP performance period have included Rebecca Wessinger, Neeraj Gupta, Jared Walker, Rod Osborne, Darrell Paul, David Ball. Additional project management support has been provided by Andrew Burchwell, Christa Duffy, Caitlin McNeil, and Jacqueline Gerst over the years.

Principal Investigator: Neeraj Gupta (614-424-3820/ gupta@battelle.org)

Report Authors and Principal Technical Contributors – Mark Kelley (Battelle), Conrad Kolb (Schlumberger) and Neeraj Gupta

Other Technical Contributors – Allen Modroo (Core Energy)

Table of Contents

List of Tables

List of Figures

Acronyms and Abbreviations

AAA	Anomalous Amplitude Attenuation
AVA	Angle vs. Amplitude
BHG	Borehole Gravity
CO_2	Carbon Dioxide
DAS	Distributed Acoustic Sensing
DOE	Department of Energy
DTS	Distributed Temperature Sensing
EOR	Enhanced Oil Recovery
FWI	Full Waveform Inversion
GAC	Geophone Accelerometer
Hz	Hertz
InSAR	Interferometric Synthetic Aperture Radar
KB	Kelly Bushing
MD	msl Depth
MRCSP	Midwest Regional Carbon Sequestration Partnership
MT	Metric Tons
NETL	National Energy Technology Laboratory
PNC	Pulsed Neutron Capture
RCSP	Regional Carbon Sequestration Partnership
RTM	Reverse Time Migration
TVD	True Vertical Depth
VSI	Versatile Seismic Imager
VSP	Vertical Seismic Profile
WHP	Wellhead Pressure

Executive Summary

A cross-well seismic survey was acquired in the Chester 16 reef from September 9 to 14, 2018 to attempt to locate 85,000 tonnes of carbon dioxide (CO_2) that were injected into the A-1 Carbonate and Brown Niagaran Formations between February 2013 and September 2018. Conducting multiple cross-well seismic surveys over time (i.e., time-lapse cross-well seismic), which includes conducting a pre-CO_2 injection (baseline) survey, has been used elsewhere to monitor CO_2 injected into the subsurface. In this study, a baseline cross-well survey was not obtained; nevertheless, it was possible to generate an image that is a plausible, albeit not without anomalies, representation of the CO_2 plume. This conclusion is supported by other monitoring and modeling results from the Chester 16 reef that provide an independent indication about the likely position of the injected CO_2.

The Chester 16 reef cross-well seismic survey was conducted between the 6-16 well, the CO_2 injection well for the Chester 16 reef, and the 8-16 well, an unperforated well located approximately 1,100 ft from the injection well that is used for monitoring. Over 19,000 (35 receiver geophones × 4 fans [positions] × 140 source locations per fan) traces were generated, which provided a dense seismic grid through the portion of the reef between the two wells. The study attempted to map the temporal change in acoustic velocity in the region between the two wells because fluid substitution involving replacement of pore fluids with CO_2 can alter the rock's velocity. This is referred to as cross-well seismic tomography because it produces images (velocity tomograms) of a vertical "slice" through the reef. Energy that propagates directly between wells without being scattered (i.e., direct arrivals) serves as the basis for constructing velocity images (tomograms). Reflection images (constructed from reflected energy rather than direct arrivals) were also produced to complement the tomograms. Reflection images illustrate reflectivity, which is a function of acoustic impedance (defined as velocity x density). Injected CO_2 can alter the reflectivity of the rock by altering both the velocity and density of the rock-fluid system. In this study, reflection images were not helpful in detecting the CO_2 plume.

The key results of the cross-well seismic survey are three figures illustrating the inferred CO_2 plume. Two figures are tomograms showing the interpreted CO_2 distribution based on the waveform tomography (i.e., full waveform inversion) results. Both figures are similar, except one is based on a source frequency of 55 hertz (Hz), (i.e., using a wavelet with frequency of 55 Hz extracted from the actual cross-well seismic data) and the other is based on a source frequency of 75 Hz. The most obvious feature in both figures is a swirl pattern representing the area where a velocity change occurred due to injected CO_2. The swirl in each figure is made up of small discontinuous areas that are interpreted to be artifacts of the finite difference wavefield modeling, not real velocity changes. This same pattern is present in the third figure is based on the reverse time migration (RTM) imaging method, as is the case with the full waveform tomography method, the RTM algorithm also uses a finite difference process that propagates a wave. While the swirls appear to be anomalous, there is at least one zone that is plausibly due to the CO_2 plume. It is an area with a velocity decrease of 400 to 600 ms that occurs in the A-1 Carbonate just above the contact with the Brown Niagaran. The location of this large velocity difference (decrease) coincides with the interval where CO_2 was injected at the 6-16 injection well. Therefore, it is possible that this velocity feature represents CO_2. Also, this result is corroborated by other monitoring results (Distributed Temperature Sensing [DTS], pulsed-neutron-capture logging [PNC], and pressure monitoring) that indicate CO_2 is present in this interval. Thus, the results include both artificial features and some results that are plausible representations of CO_2.

Several factors made this project challenging, including the deviated well geometries and the complex structure of the reef. The lack of a pre-CO_2 injection (baseline) cross-well survey was another complicating factor. To compensate for this, a pseudo-baseline velocity model was generated using pre-

injection well (sonic) logs. The Schlumberger standard cross-well seismic processing algorithm was ineffective, requiring a different approach for processing the data. As a result, an attempt was made to use an existing method for processing 3D Vertical Seismic Profile (VSP) data based on the Full Waveform Inversion (FWI) technique. The method produced results that are partially plausible, though there are ambiguities.

1.0 Introduction

1.1 Objectives of the Midwest Regional Carbon Sequestration Partnership (MRCSP) Phase III Project

The MRCSP was formed to assess the technical potential, economic viability, and public acceptability of carbon sequestration within its region. The MRCSP is one of seven regional partnerships established in October 2003 that together make up the U.S. Department of Energy's (DOE's) Regional Carbon Sequestration Partnership (RCSP) program. The RCSP program is led by DOE's National Energy Technology Laboratory (NETL).

The MRCSP Phase III Project is the Large Volume Sequestration Test Phase of the U.S. DOE Regional Carbon Sequestration Program. This program included two prior phases of study, including Phase I – Assessment of regional CO_2 emission sources and geological and terrestrial sequestration opportunities and capacity (October 2003 through September 2005) and Phase II – small-scale field sequestration demonstration tests (October, 2005 through February 2011). Phase III began May 2008 and will end at the end of 2020.

The goal of the MRCSP Phase III program is to implement a geologic injection test broad enough to promote understanding of injectivity, capacity, and storage potential in reservoir types having broad importance to the region, and, in the process, to test and demonstrate important aspects of CO_2 storage technologies to key stakeholders, These include the public, environmental groups, government officials, policymakers, and industry. The key aspects to be tested include permitting and stakeholder acceptance, CO_2 handling and compression, local transport, site assessment and development, injection and monitoring operations, site closure or transition to commercial operations, and institutional processes. Moreover, the project was required to achieve the large volume goal by injecting CO_2 continuously during several years of injection operations.

From 2013 to 2018, the MRCSP Phase III large-scale test injected over 1 million metric tons (MT) of CO_2 into a group of Silurian-age (Niagaran) pinnacle reef reservoirs in Otsego County, Michigan that are operated by Core Energy, LLC. There are over 800 pinnacle reefs in northern Michigan, and collectively, these geologic features have enough capacity to store several hundred million MT of CO_2. Moreover, most of the reefs are oil-bearing and have gone through primary production in the 1970s and 1980s. Therefore, by injecting CO_2 into the reefs, there is an opportunity to realize additional (enhanced) oil recovery (EOR) and to permanently store CO_2 after EOR. Core Energy currently operates several reefs for EOR using CO_2.

1.2 Overview of the Phase III Monitoring Program

A key objective of the MRCSP Phase III project is to evaluate the effectiveness of various technologies for monitoring CO_2 that has been injected into deep geologic formations (i.e., the Niagaran reefs). The MRCSP Phase III project included a comprehensive monitoring program in parallel with injecting over 1 million tonnes of CO_2 into a subset of ten (10) Niagaran pinnacle reefs operated by Core Energy. Figure 1-1 and Table 1-1 identify the monitoring technologies conducted at each of 10 pinnacle reefs. The monitoring program included the following:

- At all 10 reefs, a basic monitoring suite consisting of CO_2 mass-balance accounting (i.e., injection rate, cumulative CO_2 injected, production rate, cumulative CO_2 produced) and reservoir pressure.

- At the Dover 33 reef, six additional monitoring techniques including VSP monitoring; geochemistry monitoring; borehole gravity (BHG) monitoring; PNC logging; satellite monitoring (InSAR – Interferometric Synthetic Aperture Radar); and micro-seismicity monitoring.
- At the Bagley reef and the Charlton 19 reef, two additional monitoring techniques including geochemistry monitoring and PNC logging.
- At the Chester 16 reef, five additional monitoring techniques, including Distributed Acoustic Sensing (DAS) VSP monitoring; cross-well seismic monitoring; DTS; geochemistry monitoring; and PNC logging.

Eleven (11) separate reports have been prepared for the 11 monitoring technologies listed in Table 1-1. Each report discusses the objectives of the monitoring study, methods that were used for measuring/evaluating the effectiveness of the monitoring technology, and results of each monitoring technology. This report discusses the cross-well seismic monitoring technology that was implemented at the Chester 16 reef.

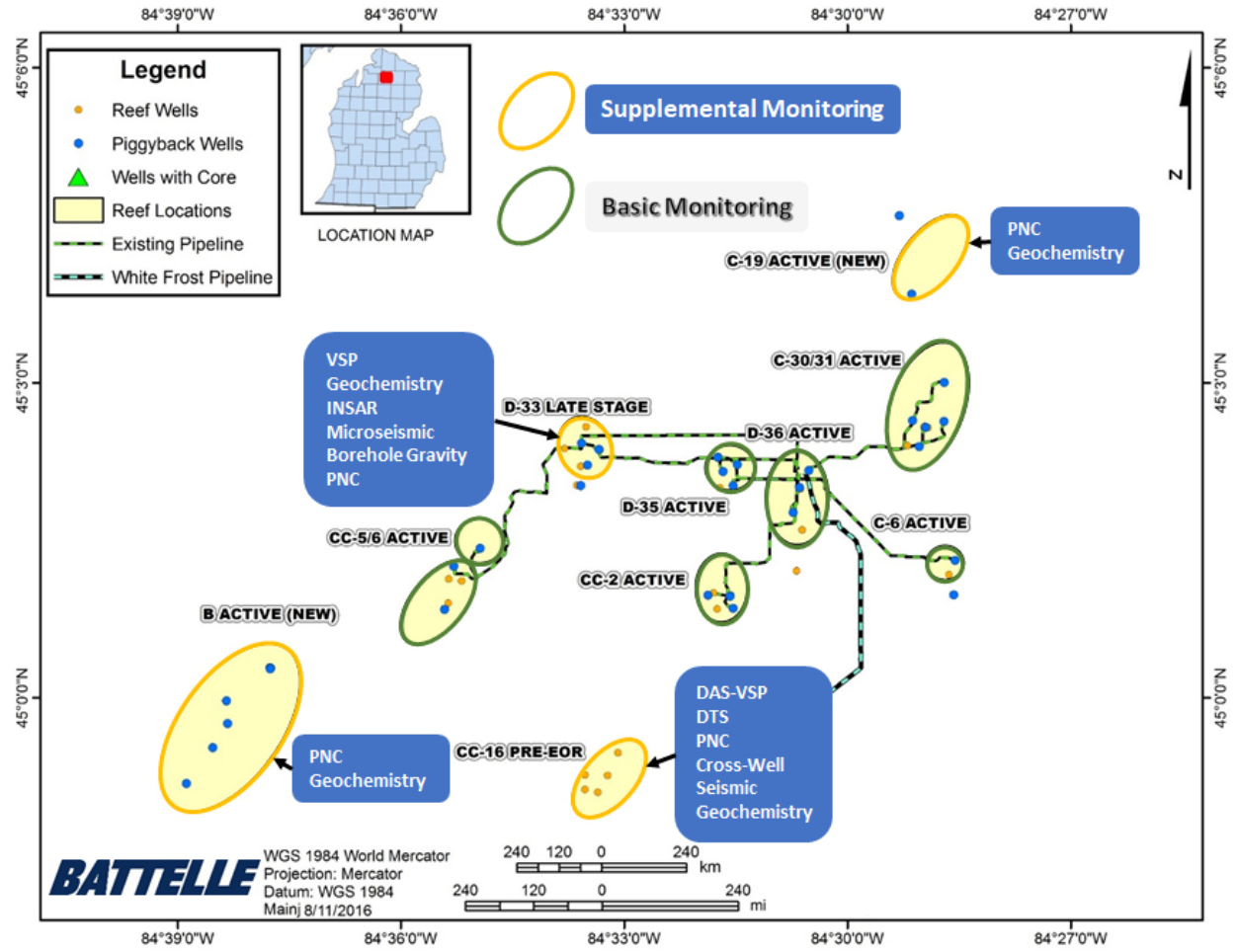

Figure 1-1. Monitoring Methods Employed at Various reefs during the MRCSP Phase III Program.

Table 1-1. Monitoring Technologies and Objectives as Implemented by Reef

	Monitoring Objective				Monitoring by Reef				
Monitoring Technology	Mass-Balance Accounting	Leak Detection/ Well Integrity	CO_2 Plume Tracking/ Interaction	Induced Seismicity, Uplift	Dover 33	Charlton 19	Chester 16	Bagley	Other reefs
CO_2 injection/ production	X				X	X	X	X	X
Reservoir Pressure		X	X		X	X	X	X	X
Temperature (DTS)		X	X				X		
PNC logging		X	X		X	X	X	X	
Borehole gravity			X		X				
Geochemistry			X		X	X	X	X	
Vertical seismic profile[a]		X	X		X		X		
Cross-well seismic			X				X		
Microseismicity				X	X				
InSAR (Satellite radar)				X	X				

[a] Two varieties of VSP were implemented, including conventional VSP using geophones conveyed on a tubing string (Dover 33) and DAS VSP using fiber optic cable permanently mounted to the outside of the deep casing string (Chester 16).

1.3 Description of Cross-Well Seismic Profiling

Cross-well seismic profiling is a form of borehole geophysics that is conducted between a pair of wells with the source (tool) and receiver (array) each placed inside one the wells, as illustrated in Figure 1-2. In cross-well seismic imaging, a seismic source is placed in a wellbore and receivers in a nearby wellbore to provide high resolution images and estimates of reservoir properties between the wells (Figure 1-2). The receiver array is held fixed in one well while the source tool is moved upwards in the other well in small increments, whereby at each position the source tool is "activated." A typical survey will involve numerous source points spanning the target interval. After one complete source run, the receiver array is repositioned (moved up by some specified distance that is less than the distance between geophones) and the source run is repeated. The advantages of cross-well imaging over surface seismic include the dramatic increase in available resolution in reflection imaging and the ability to directly measure a 2-D velocity field using tomography.

Travel time tomography, which is based on ray tracing, uses only the direct arrival times (illustrated in Figure 1-1) and the well deviation data to determine a velocity model. The distance each raypath travelled through each layer of the model and the total time from source to receiver is combined and used to solve for the best fit velocity value for each of the model layers. While this method has historically produced good results, it doesn't use other information embedded within the trace data. For example, it only uses direct arrivals and ignores up-going or down-going reflections and refractions. ***Full waveform tomography*** (FWI) attempts to use not only direct arrivals but also reflections, refractions, and other information to solve the velocity model. It starts with an initial velocity model and then adds detail by propagating a wavelet through the initial model using a finite difference algorithm. The difference between

the predicted trace dataset and the observed (i.e., acquired) trace data set provides a residual dataset that shows the amplitude differences between the two datasets, indicating error in the model.

The distance between the source and receivers (i.e., the well spacing) is considerably less than the propagation distances associated with surface seismic methods. This allows the use of much higher source frequencies than what is used with surface seismic methods, resulting in a significant increase in spatial resolution. Cross-well surveys can employ a frequency band between 20Hz and 2000 Hz, depending on the type of source used, the distance between wells, and the attenuation characteristics of the zone under investigation. Resolution on the order of 10 feet (3 meters) is possible. The resolution of cross-well reflection imaging in carbonate reservoirs has been demonstrated to be 10 times or greater than that of surface seismic data, with vertical resolution of 5 to 10 feet.

Cross-well processing is like surface seismic processing in that it includes velocity estimation (tomography) and reflection imaging. Reflection imaging usually provides more resolution than the velocity image (tomogram) but depends critically on the accuracy of the velocity model for good results. One disadvantage of the cross-well method is that it is 2-D.

Reverse Time Migration (RTM) is an advanced **migration** method for **seismic** depth imaging. The strength of RTM is that it fully respects the two-way acoustic wave equation, thus improving imaging in areas where complex geology violates the assumptions made in Kirchhoff or one-way wave equation migrations.

Monitoring changes in reservoir conditions (e.g. saturation or pressure) using cross-well usually requires multiple visits to the same site in order to obtain time-lapse images. In this study, a baseline (pre-CO_2 injection) cross-well survey was not obtained; however, the injected CO_2 was successfully delineated with a single cross-well survey after 85,000 tonnes of CO_2 had been injected.

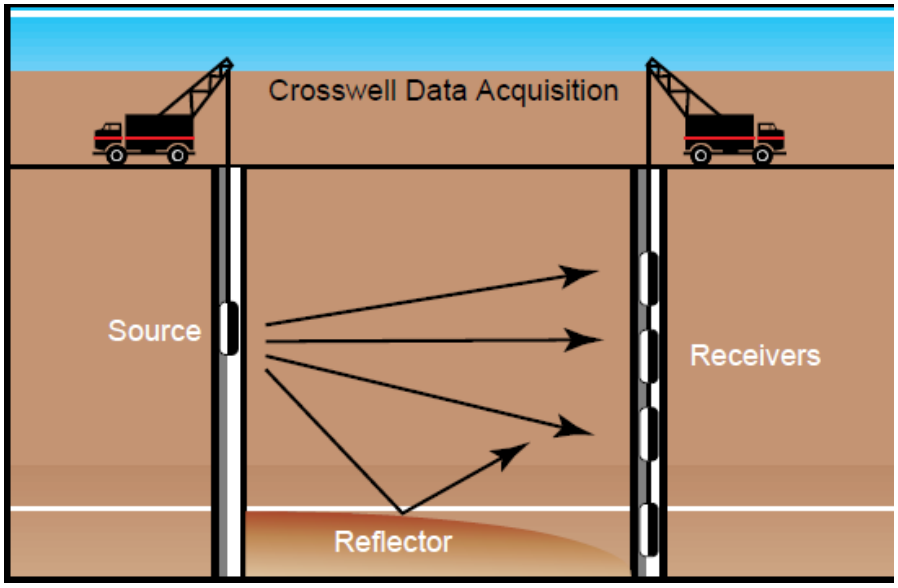

Figure 1-2. Cross-well data are collected by placing a seismic source in one well and a receiver string in a nearby well. Energy that propagates directly between wells without being scattered (i.e., direct arrivals) serves as the basis for constructing velocity images (tomograms). Energy that is reflected is used to construct reflection images (source: Harris and Langan (2001)).

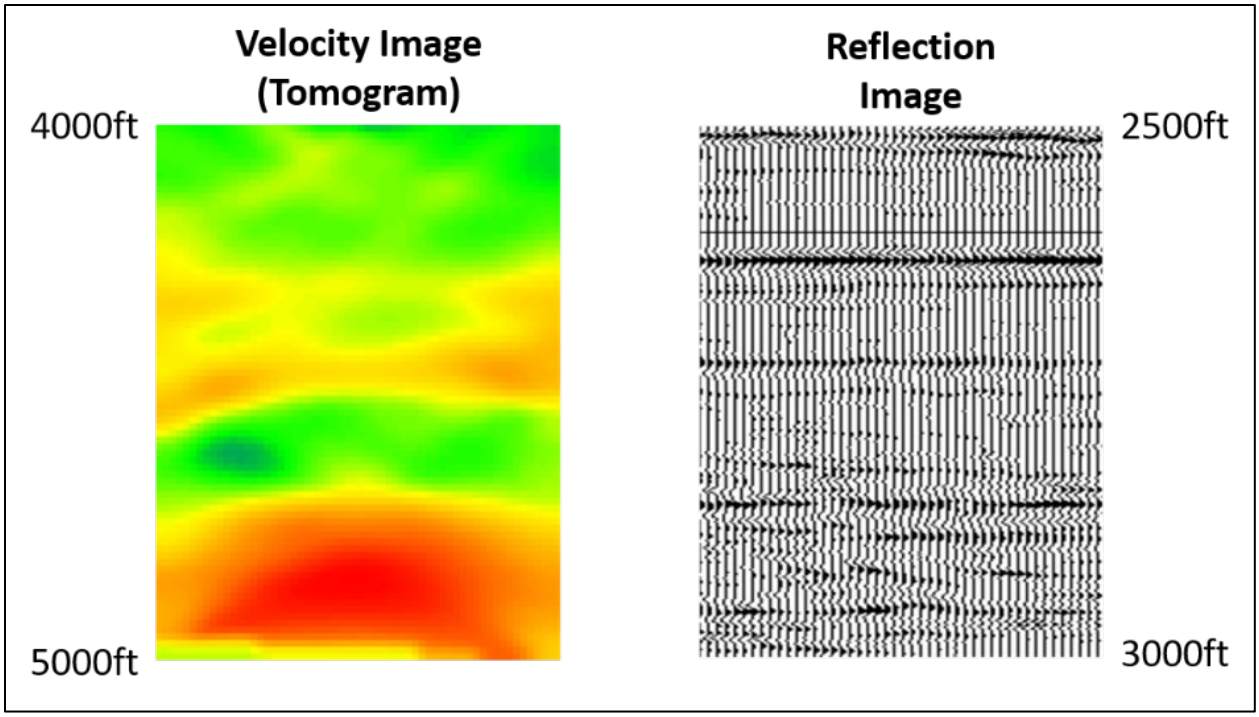

Figure 1-3. Two representations of cross-well data.

2.0 Data Acquisition

The Chester 16 reef cross-well seismic survey was conducted between the 8-16 well and the 6-16 well, both installed in late 2016. The 6-16 well is the CO_2 injection well for the Chester 16 reef and the 8-16 well is, as of this report, an unperforated well that has been used for monitoring CO_2 using various technologies including DAS VSP (see companion monitoring reports), distributed temperature sensing (see companion monitoring report), pressure monitoring using externally mounted gauges (see companion monitoring report), and pulsed neutron capture logging (see companion monitoring report). Both wells are deviated as shown in Figure 2-1. The geologic layers penetrated by each well and their depths in measured feet and elevation relative to sea level are given in Table 2-1. Surface coordinates for each well are provided in Table 2-2.

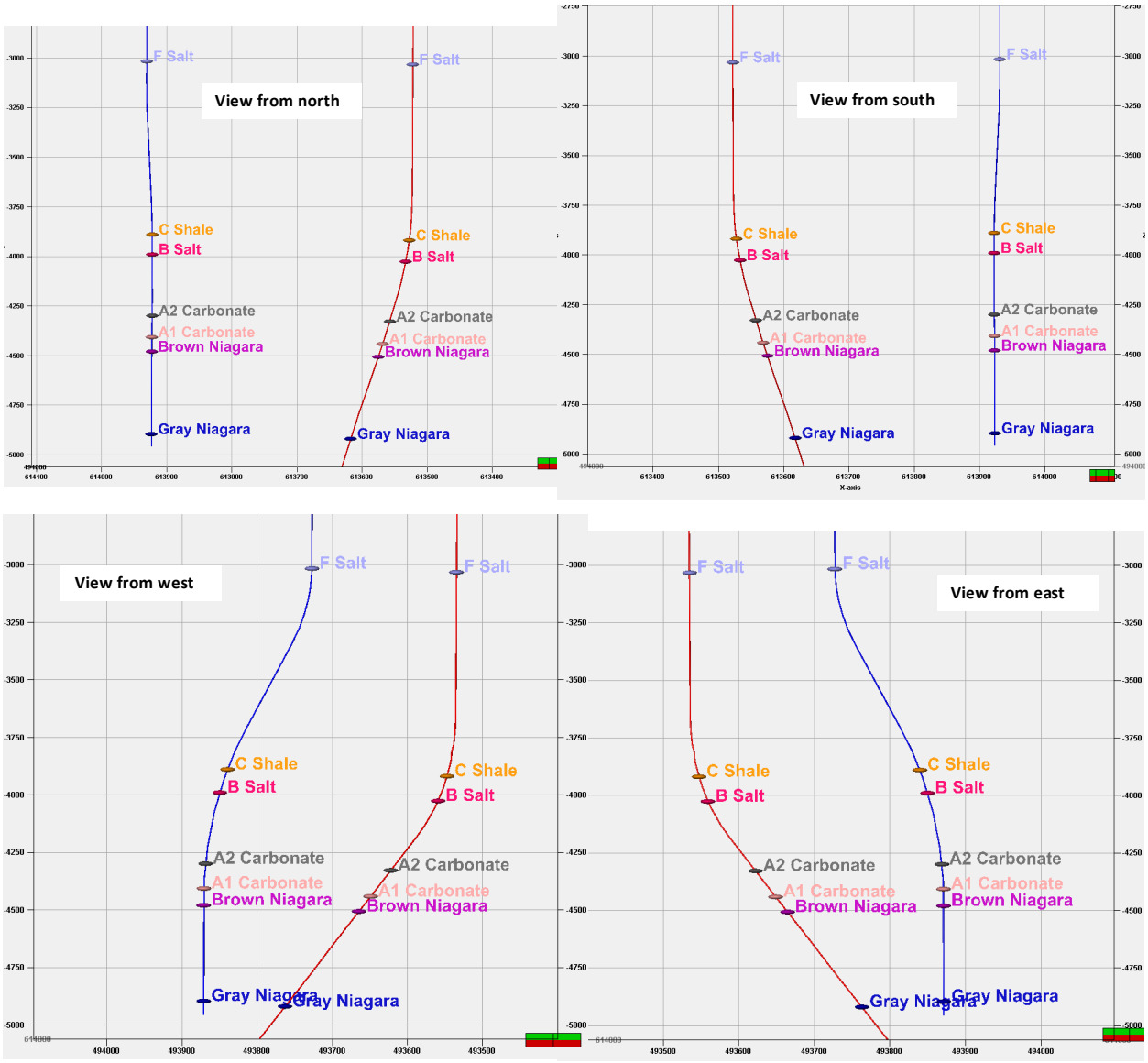

Figure 2-1. Trajectory of the 6-16 Source well (red) and the 8-16 Receiver well (blue). Units on Y-axis are feet relative to sea level and units on X-axis are feet (MichiganGeoRef83 (Code: 501480) coordinate system).

Table 2-1. Formation Contacts for each Well

	6-16 Well		8-16 Well	
Name	Elev. TVD (ft msl)	Depth (MD ft)	Elev. TVD (ft msl)	Depth (MD ft)
Reference Elevation	K.B. 1321.0	0	K.B. 1338.0	0
Base of Drift	464.00	857.00	465.05	873.00
Antrum	-153.95	1475.00	-136.30	1475.00
Dundee	-1041.89	2363.00	-1032.79	2372.00
Bois Blanc	-2171.31	3493.00	-2151.43	3491.00
Bass Island	-2628.27	3950.00	-2615.38	3955.00
F Salt	-3032.24	4354.00	-3016.36	4356.00
C Shale	-3918.63	5245.00	-3889.38	5313.00
B Salt	-4026.23	5361.00	-3989.86	5419.00
A-2 Carbonate	-4328.10	5737.00	-4299.18	5735.00
A-1 Carbonate	-4441.00	5884.00	-4406.88	5843.00
Brown Niagara	-4506.40	5970.00	-4479.87	5916.00
Gray Niagara	-4919.46	6513.00	-4895.87	6332.00

Table 2-2. Location Information for each Well

Well Name	Reference Elevation (ft)	Northing (m)	Easting (m)
6-16	K.B. 1321.0	493519.93	613517.80
8-16	K.B. 1338.0	493745.30	613916.80

Coordinate system: MichiganGeoRef83 (Code: 501480)

The data was acquired by conducting five passes (fans) with the source tool in the 6-16 well, each time revisiting the same source depth points, across a 1,930-ft long interval extending from 4560 ft MD to 6490 ft MD in the 6-16 well. This interval spans 685 feet of the F-Salt and extends through 520 feet (out of 543 feet) of the Brown Niagaran (Table 2-1). The source tool was activated every 10 feet during each pass, resulting in approximately 140 source activations per pass. The receiver array contained 35 geophones spaced 50 ft apart and spanned a 1,700 ft long interval that extends from 205 feet below the top of the F-Salt through 385 feet of Brown Niagaran (out of 416 feet). For each consecutive source run, the receiver array was moved up 10 feet in the 8-16 well. Therefore, the effective receiver spacing, after combining all five fans, was 10 feet rather than the geophone spacing of 50 feet. This is illustrated in Figure 2-2. Source acquisition parameters are summarized in Table 2-4 and Table 2-5.

Table 2-3. Fan Measured Depths

Fan Number	Date	Receiver Min (MD)	Receiver Max (MD)	Source Min (MD)	Source Max (MD)
1A,1B,1C	9/12/18	4601	6301	4560	6490
2A,2B	9/13/18	4591	6291	4560	6490
3A,3B	9/13/18	4581	6281	4550	6490
4A,4B	9/13-14/18	4571	6271	4560	6490
5A,5B	9/14/18	4561	6261	4560	6490

Table 2-4. Source Acquisition Parameters

Parameter	Value	Units
Source Tool	Z-Trac	N/A
Receiver Tool	VSI-35	N/A
Receiver Level Spacing	50 (10)[a]	feet
Source Level Spacing	10[b]	feet
Stack	4[c]	traces
Sample Period	1	milliseconds
Record Length	1	seconds
Sweep Length	11.6	seconds
Dead Time	3.0	seconds
Sweep Start Frequency	30	Hertz
Sweep End Frequency	400	Hertz

a. *Geophone spacing on 35-level Versatile Seismic Imager (VSI) array is 50 ft (span length of array is 1700 ft); the effective geophone spacing is 10 ft when all five interleaved fans are combined)*

b. *Source interval was 4550-6490 for upper axis (p-wave) and 4570-6510 for bottom axis (s-wave). After rotation there will be traces for all levels at which both upper and lower axis were shot, or 4570-6490 feet re kelly bushing (KB), or 192 source levels.*

c. *Stack refers to number of source shots per level, per axis*

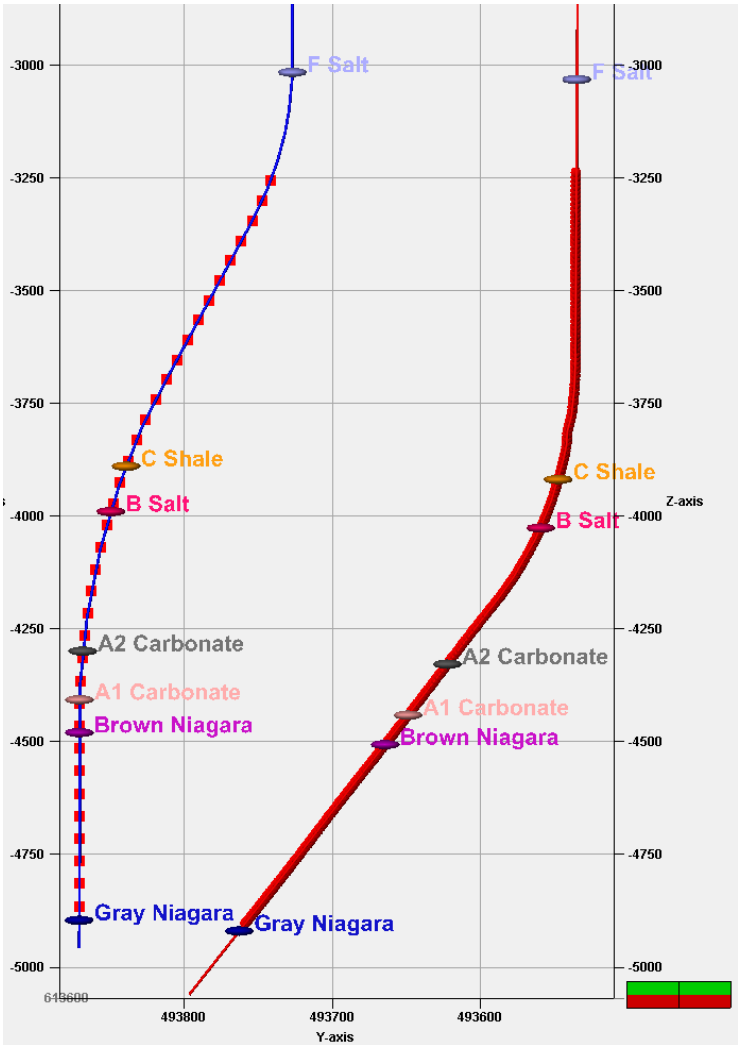

Figure 2-2. Fan 1 Receiver positions (left) and source activation points (right)

Pre-job modeling was performed to design the cross-well survey prior to acquiring the data. The target interval for imaging CO_2 is a 400-ft thick interval from 5800 to 6200 ft MD, which spans all the A-1 Carbonate and the upper 230 ft (6-16 well) to 284 ft (8-16 well) of the Brown Niagaran. This interval also encompasses four of the five perforated intervals in the 6-16 injection well (Figure 2-3; Table 2-5).

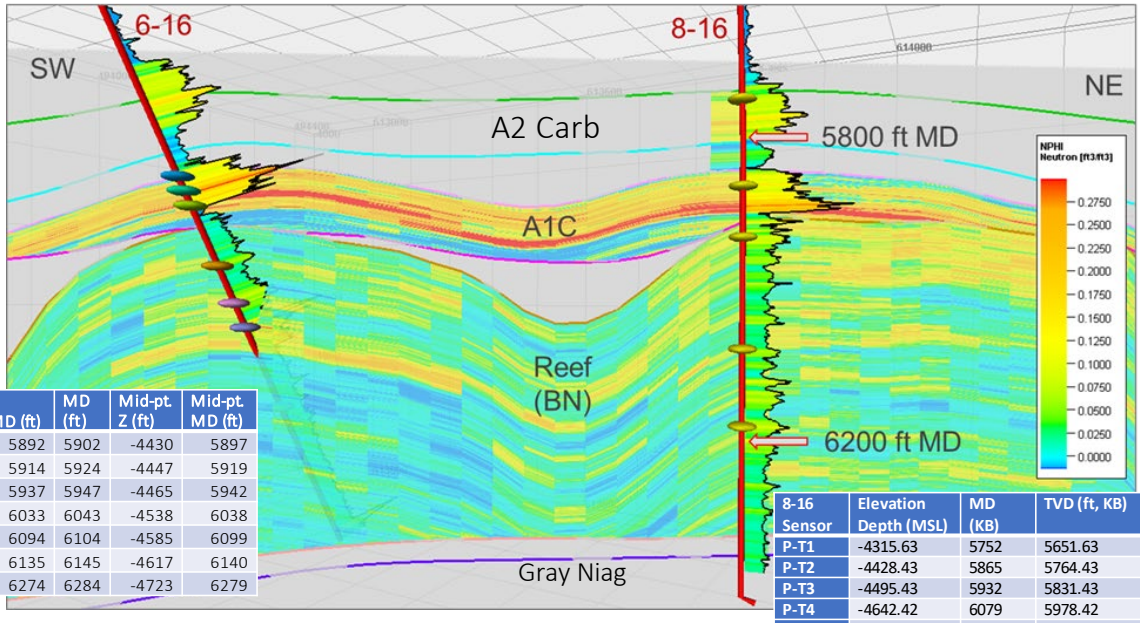

6-16 Perf Interval	MD (ft)	MD (ft)	Mid-pt. Z (ft)	Mid-pt. MD (ft)
Perf 1	5892	5902	-4430	5897
Perf 2	5914	5924	-4447	5919
Perf 3	5937	5947	-4465	5942
Perf 4	6033	6043	-4538	6038
Perf 5	6094	6104	-4585	6099
Perf 6	6135	6145	-4617	6140
Perf 7	6274	6284	-4723	6279

8-16 Sensor	Elevation Depth (MSL)	MD (KB)	TVD (ft, KB)
P-T1	-4315.63	5752	5651.63
P-T2	-4428.43	5865	5764.43
P-T3	-4495.43	5932	5831.43
P-T4	-4642.42	6079	5978.42
P-T5	-4744.42	6181	6080.42

Figure 2-3. Porosity cross-section showing depth of the 7 perforated intervals in the 6-16 well relative to the target imaging interval.

Two well configuration scenarios were evaluated in the pre-survey modeling analysis. One scenario assumed a bridge plug would be placed in the 6-16 source well just above the perforations for pressure control—the implication of placing a bridge plug in the well is that it would limit the maximum depth that the source tool could reach. This scenario was considered undesirable, due to loss of data coverage. Therefore, a second scenario was evaluated that assumed a wellhead lubricator would be used to control pressure, in which case a bridge plug would not be required. This allowed the source tool to be lowered into the well as deep as necessary to optimize coverage of the target interval. Figure 2-4 shows the estimated data coverage in cross section and plan view for the second scenario (without a bridge plug).

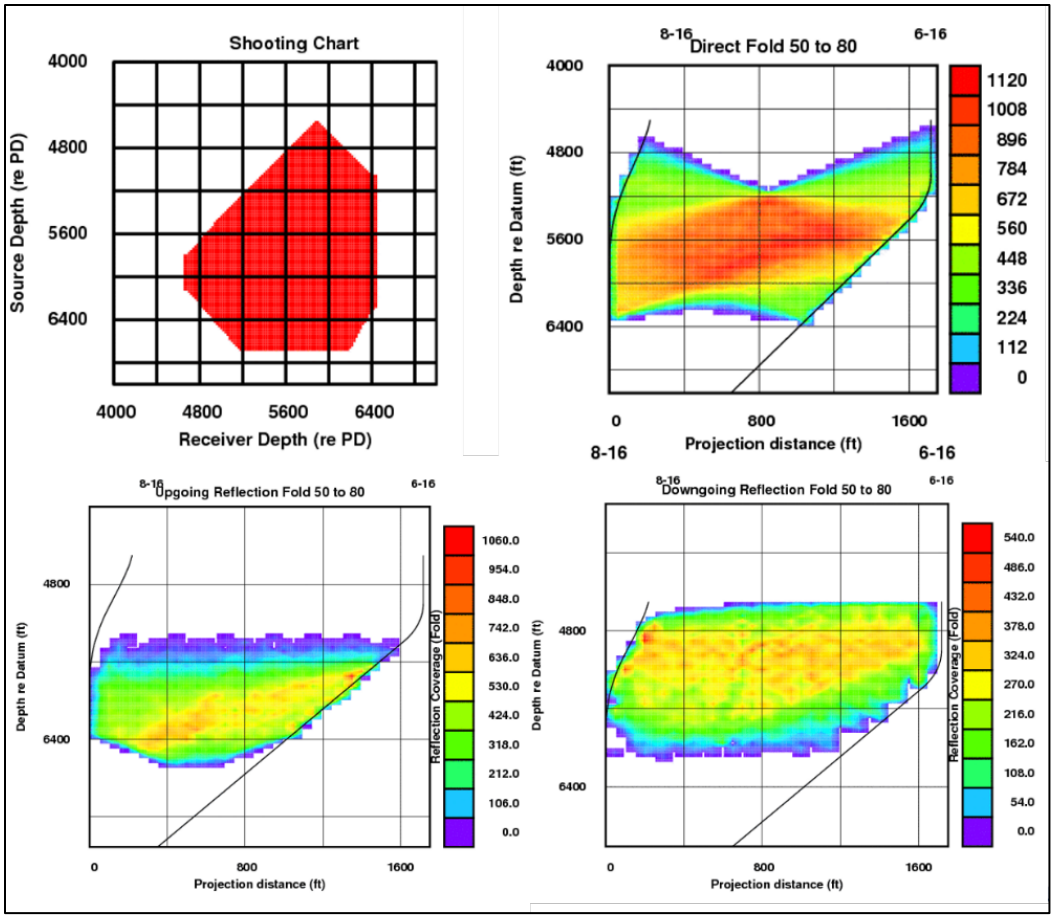

Figure 2-4. Results of Pre-job Modeling showing Estimated Data for the Scenario without a Bridge Plug in the 6-16 Source well.

Table 2-5. Parameters used in Pre-Job Modeling

Parameters
Source well: 6-16
Receiver well: 8-16
Source well head pressure>0 (Full lubricator assumed)
Receiver tool: (35 Levels @50 ft spacing); @1ms sampling rate
Receiver x Source = 10x10 ft
Well spacing: 1500 feet
Interval of interest: 5800 to 6200 feet MD
Sweep frequency: 30 to 400 hz
Sweep seconds: 46.4 sec/level

Schlumberger has two source tools, including Z-Trac with frequencies of 30 to 800 Hz, and X-series with frequencies of 100 to 2000+ Hz. Z-Trac was selected for this project due to its greater energy output and magnetic clamping. The X-Series source is fluid coupled so S-wave data may not be obtained. The Z-Trac can impart a large amount of energy into the formation by sweeping frequencies in the range of 30-800 Hz, which reportedly allows enhanced seismic imaging between wells up to 2km apart. In addition, the tool can generate both compressional and shear wave energy simultaneously. The source tool is magnetically clamped and is intended specifically for formations with high attenuation and large distances between wells. Operating at a lower frequency range (30-800 Hz), this source produces about 20 dB more amplitude than current piezoelectric sources. It also produces both direct compressional and shear energy waves, allowing for advanced wavefield analysis. It distributes the energy produced over an area in the wellbore that is 10 to 13 feet in length, which is large enough not to cause damage to the casing or cement. The expected resolution of the cross-well seismic technology at the Chester 16 site is equal to λ (shortest wavelength)/4, where λ is equal to rock velocity (20,000 ft/sec)/source frequency (400 Hz [s-1]). This yields a resolution of 12.5 ft. This indicates geologic features (e.g., individual beds) thicker than 12.5 ft can be imaged.

Although the Z-Trac source can generate frequencies from 30-800 Hz, a smaller range was realized in this study. By the Nyquist sampling theorem, the maximum frequency that can be preserved without aliasing (distortion of frequency introduced by inadequately sampling) is 1/(2*DT) where DT is the sample period (Nyquist frequency, equal to twice the maximum frequency in the signal). For a 1 ms sampling period, the Nyquist frequency is 500 Hz. Any energy above that frequency will be aliased and adds noise into the frequency band below 500 Hz. To prevent this, acquisition systems have anti-alias filters built in that ensure energy above the Nyquist frequency is not recorded. These anti-alias filters are typically set at 0.6-0.8 of the Nyquist frequency. For the Versatile Seismic Imager (VSI) system, the threshold is at 0.8 Nyquist, or 400 Hz. In order to recover higher frequencies, a smaller sample period would be needed, e.g. 0.5 ms. This would have limited the VSI receiver array to 20 levels, versus the planned 35 levels, and increased the survey duration by almost a factor of 2.

Figure 2-4 shows a spectral analysis of the frequency domain for one source station. Frequency output slowly ramps-up in amplitude from 30 Hz to approximately 250 Hz. The cause of the amplitude reduction in the low frequencies was the high inclination of the source well. The very heavy tungsten source tool was not able to achieve enough amplitude in the inclined portion of the source well when it was operating at these low frequencies. These low amplitude frequencies were corrected during processing. Maximum source frequency was 400 Hz.

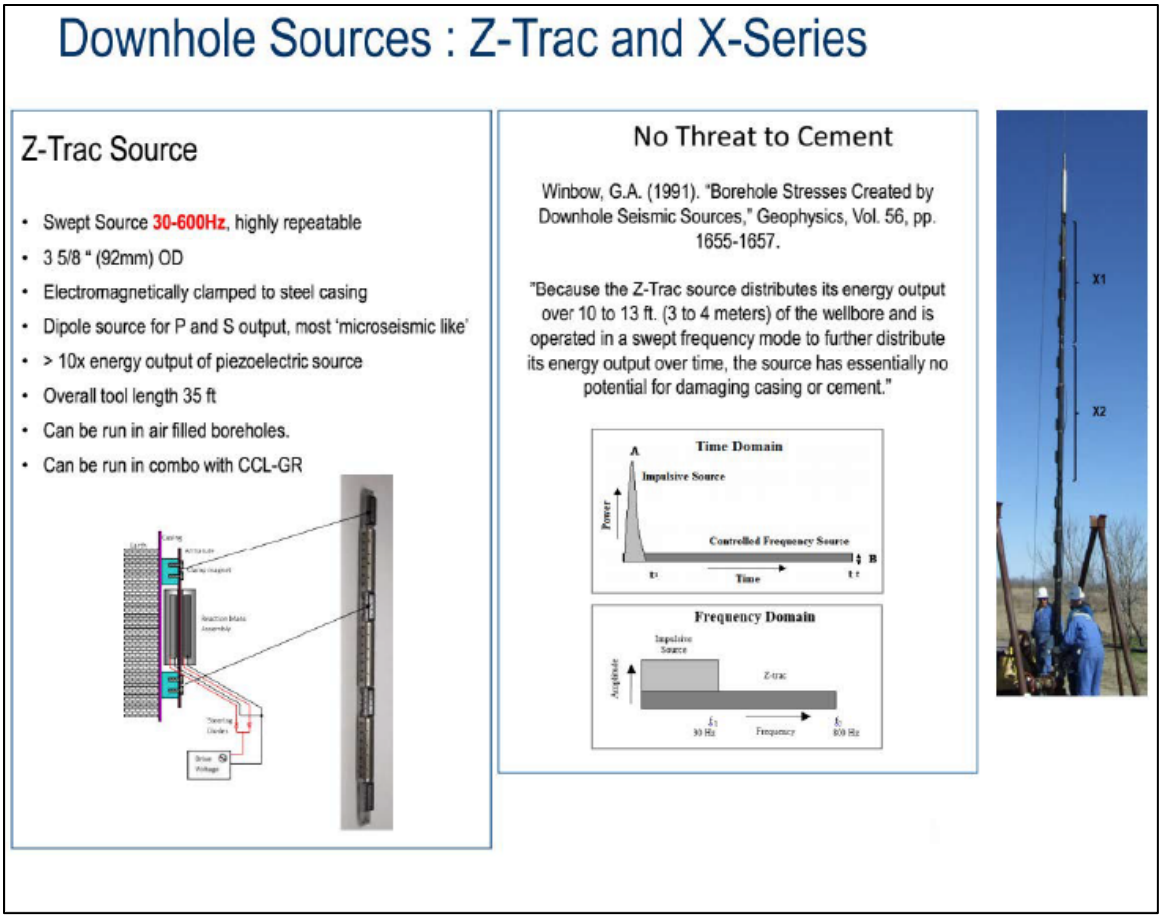

Figure 2-5. Details of the Schlumberger Z-Trac Seismic Source Tool used in this study

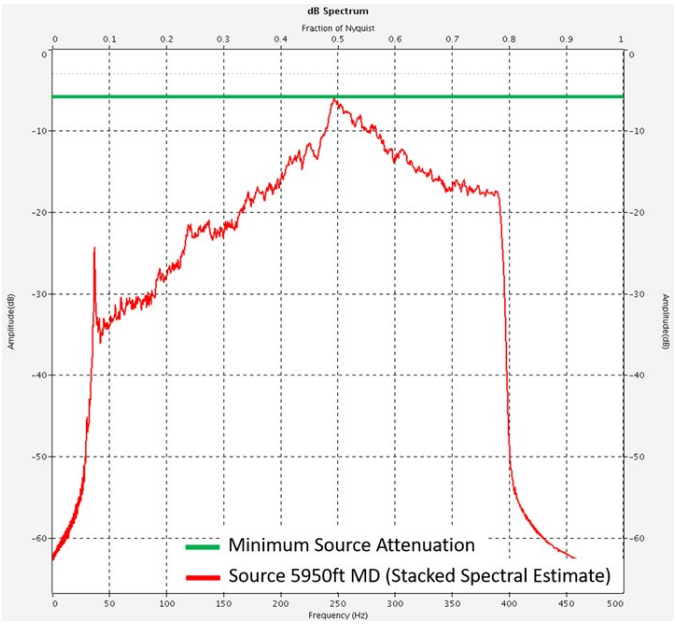

Figure 2-6. Raw Data Frequency Spectrum (Fan 5A Source 5950 ft MD)

For recording the cross-well survey, Schlumberger used their VSI downhole microseismic monitoring array. The VSI tool is usually run in a 12-shuttle (i.e., 12 level) configuration, but can be also be run with 20 or more shuttles, with the vertical distance between shuttles being either 50 ft or 100 ft, depending on pre-survey modeling results. For this project, a 35-level array with a 50-ft spacing was used.

Each shuttle contains a sensor package that is mechanically decoupled from both the shuttle itself and the rest of the tool string. This allows for low noise, resonance-free recording. The VSI sensor package contains Schlumberger developed proprietary three-axis omni tilt geophone accelerometers (GAC) that are specifically designed for borehole seismic recordings. The VSI downhole seismic sensor measures particle motion of the formation at the wellbore. The VSI tool uses Q-Technology®, single-sensor seismic hardware and software and advanced wireline telemetry for efficient data delivery from borehole to the surface. The VSI tool (array) was conveyed into the 8-16 well via wireline.

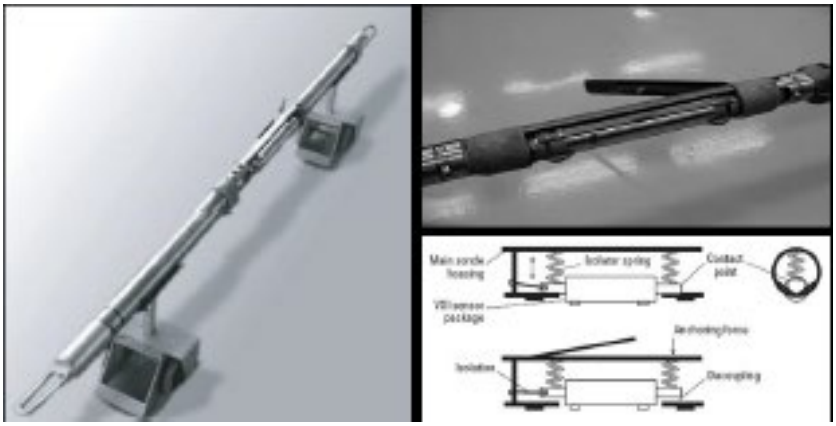

Figure 2-7. VSI Sensor

3.0 Cross-Well Seismic Tomography

Cross-well seismic tomography measures the two-dimensional velocity field (at seismic frequencies, usually in the frequency range of 20 Hz to as high as several kilohertz) between wells. The velocity field is usually represented by a color-coded map referred to as a *tomogram,* in which a color is assigned to the seismic velocity at each point. Cross-well tomographic data is processed using algorithms that simultaneously reconstruct both the seismic velocity field of the reservoir, as well as the path of the energy through it. Algorithms based on ray tracing or some form of the wave equation are usually used. These algorithms solve a system of nonlinear equations to reconstruct the velocity field between the boreholes for compressional and/or shear waves.

This section provides a brief summary of the process of producing tomograms and presents resulting tomograms. The processing workflow to produce velocity tomograms involved several steps, as shown in Figure 3-1. This section presents a series of figures illustrating the process and results of cross-well seismic tomography – i.e., generation of p-wave and s-wave velocity maps (tomograms) for the interwell region using the standard Schlumberger velocity inversion method.

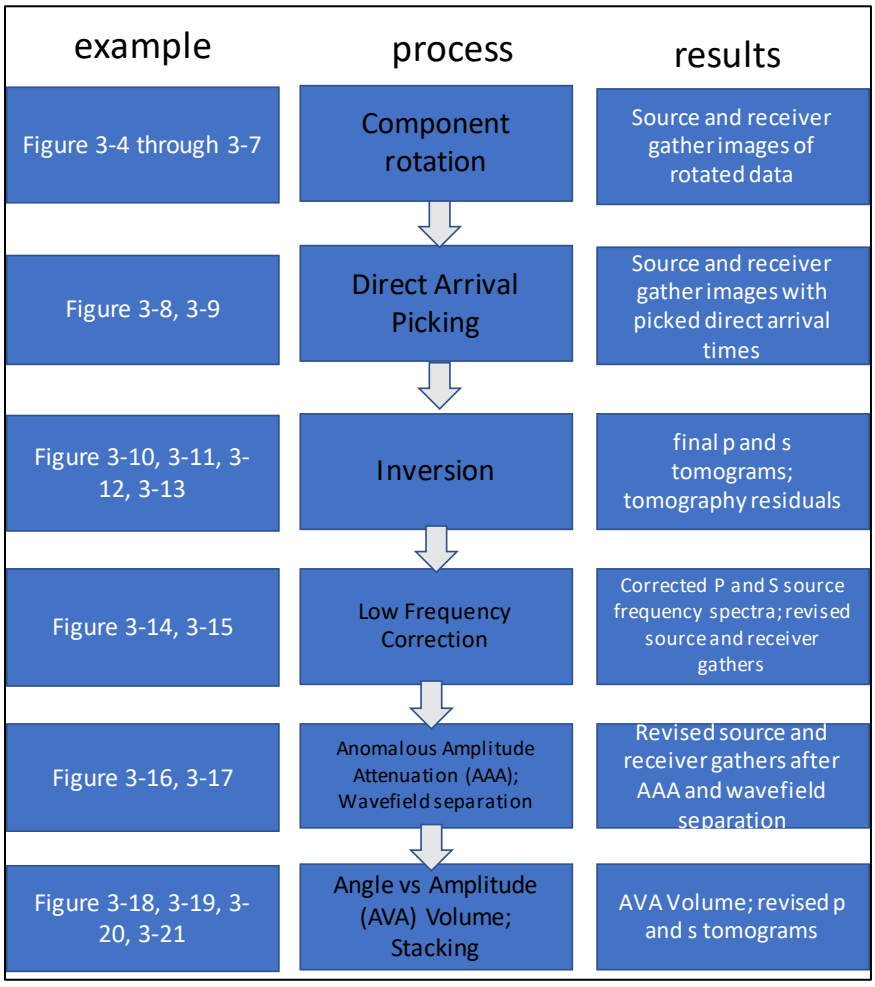

Figure 3-1. Cross-well seismic Tomography Workflow.

The standard cross-well (velocity) inversion method (travel time tomography) uses only the well deviations and first arrival travel-time picks to invert for the layered, (polynomial-basis) velocity tomogram. The algorithm begins with a constant velocity model and uses a relaxed ray tracing to determine travel-time residuals between the ray-traced times and the actual times. The next ray tracing iteration attempts to minimize the travel-time residuals, initially solving the low spatial frequencies, with each subsequent iteration hopefully increasing the resolutions of the resulting tomogram while decreasing the residuals.

The inversion algorithm uses a third-order Chebyshev polynomial basis to solve the velocity field, which reduces the degrees of freedom to nine. This reduction in parameters allows the inversion to solve for the velocity utilizing only the well deviation data and the direct-arrival picks. The disadvantage of this choice of parameterization is a loss of horizontal resolution, since the velocity change is limited to a maximum that is within the third-order polynomial bounds. Nevertheless, the polynomial-based inversion can reportedly identify a minimum velocity change of 1-2% provided the velocity anomaly is large enough to affect several raypaths and be identifiable in direct-arrival picks. Figure 3-2 shows the point set of the polynomial structural model used for the velocity inversion. The inversion has six fundamental parameters that can be adjusted to invert for the velocity model, which can be grouped into either velocity or anisotropy control. The velocity group of three parameters are dampening factors to control how quickly the inversion can change in the inline, crossline, or vertical direction. The three anisotropy parameters control the amplitude, rate of change, and vertical independence of the Thomsen eta and epsilon parameters.

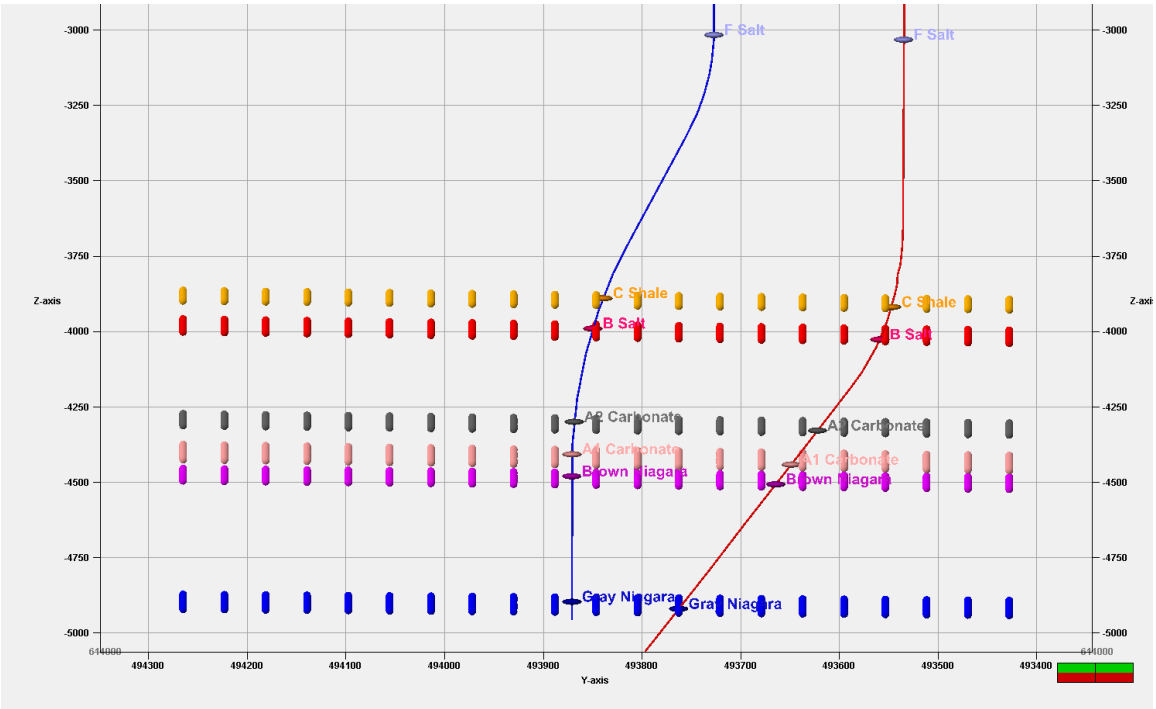

Figure 3-2. Chebyshev Polynomial Structural Model (View from west)

The Schlumberger cross-well tomographic (and imaging) algorithms, being fully 3D, require a projection plane to view the velocity field and the reflection image. In this study the A-1 Carbonate was selected to serve as the project plane because it is one of two CO_2 injection intervals (the upper Brown Niagaran is also an injection interval, as shown in Figure 2-3). Figure 3-3 illustrates the chosen, best fit plane, that aligns with the A-1 Carbonate horizon.

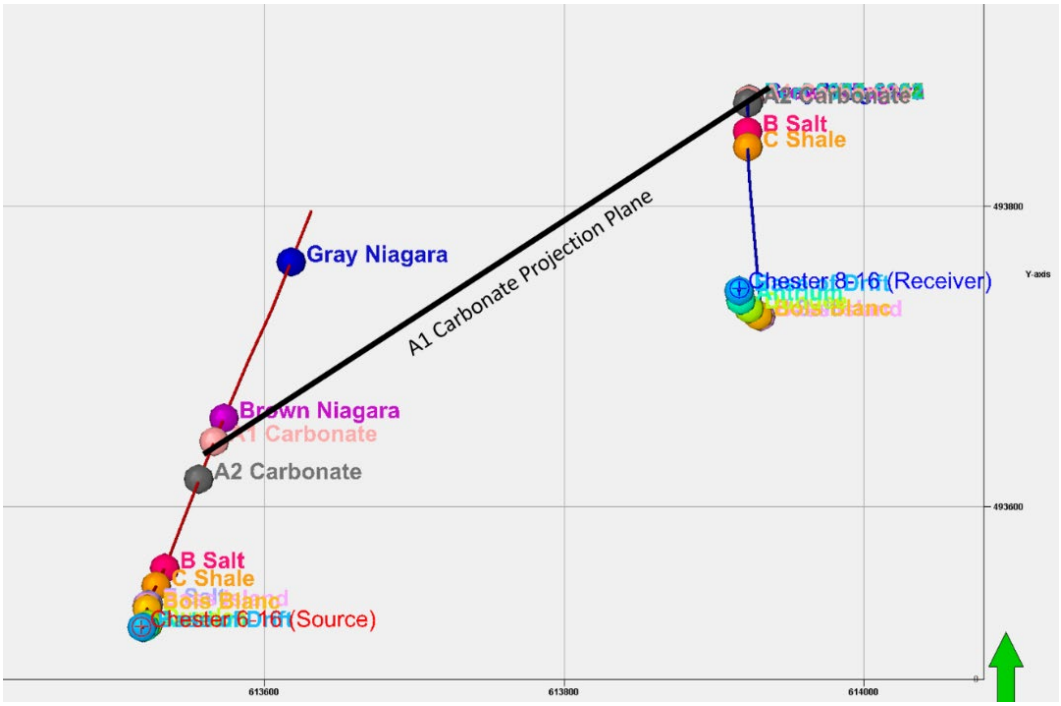

Figure 3-3. A-1 Carbonate Projection Plane

The tomography results are presented in Figure 3-10 and Figure 3-12, which show results of the polynomial-basis tomography utilizing the A-1 Carbonate projection plane. These figures also show sonic logs in black, overlaid with the tomography result in blue. Both figures show good correspondence with the well logs, particularly the shear wave. The result from the shear tomography (Figure 3-12) can capture the velocity reduction for both the CO_2 injection at the A-2 Carbonate and the Brown Niagaran.

The polynomial-basis tomography does accurately describe the velocities near the wellbore, but due to the limited structure and horizontal resolution inherent in the polynomial scheme, the results are limited in how well they can accurately describe the true geology. While a 3rd order polynomial can describe a flat, dipping, or anticline/syncline structure, the polynomial is less capable of describing the complex structure in the Chester 16 reef, thus limiting the accuracy of the subsequent inversion and imaging. The 3rd order polynomial is not only the basis of the gross structure of the area, it is also the basis of the tomographic solution. For most applications, the velocity polynomial can solve for smooth gradual changes in velocity between the wellbores. Abrupt velocity variations (i.e. large offset faults, CO_2 injection, etc.) within the profile pose a significant challenge to the standard inversion algorithm, due to the polynomial basis imposing a smoothly varying and continuous solution. The traditional cross-well workflow is also limited by its dependence on an imaging projection plane.

Because these limitations are within the standard cross-well workflow, a novel workflow using FWI and RTM was necessary. Both these algorithms, while routinely used in 3D VSPs and surface seismic, had not previously been applied to cross-well seismic data by Schlumberger. These methods are discussed in

Section 4 of this report. The remainder of this section presents intermediate processing products and final processing results of the tomography inversion process, following the workflow presented in Figure 3-1.

3.1 Component Rotation

Figure 3-4 through Figure 3-7 show examples of source and receiver gather images of rotated p-wave and s-wave data. Depths are listed in true vertical depth (TVD).

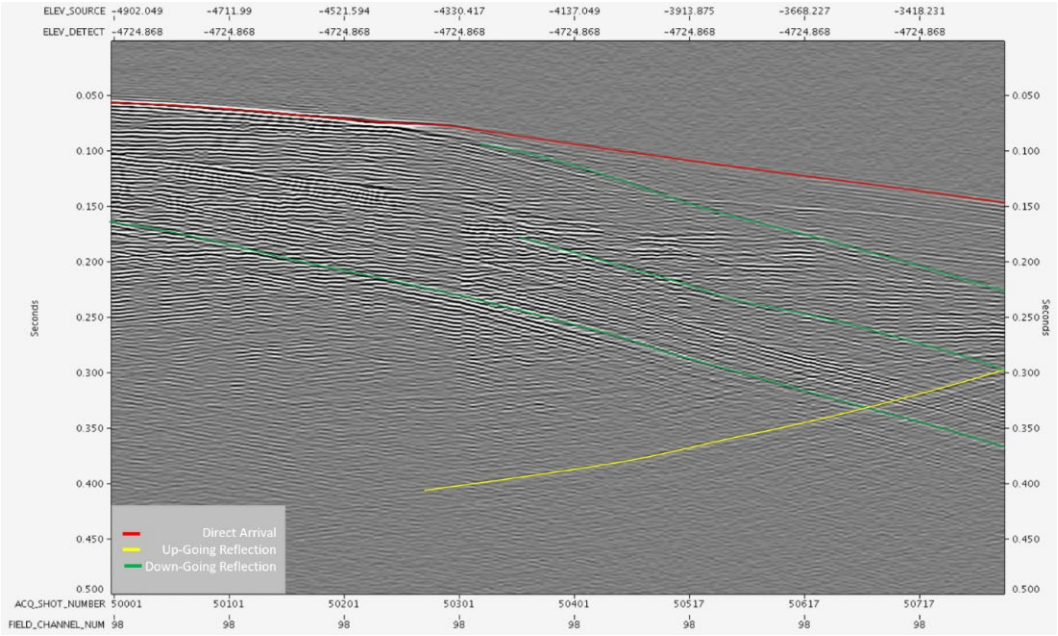

Figure 3-4. Example Compressional Receiver Gather (TVD -4724.87m)

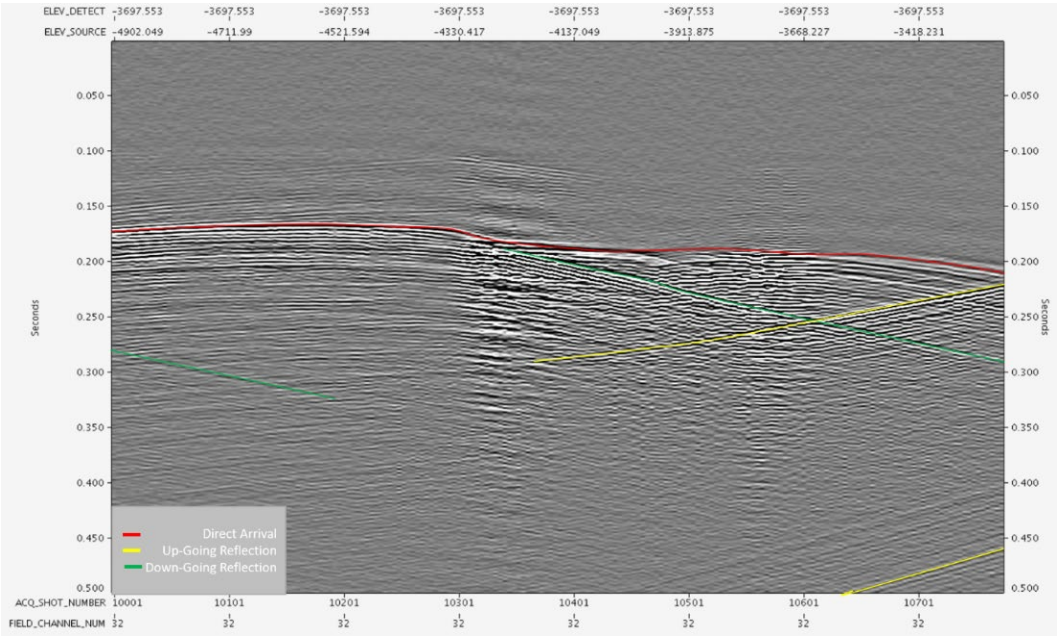

Figure 3-5. Example Shear Receiver Gather (TVD -3697.55m)

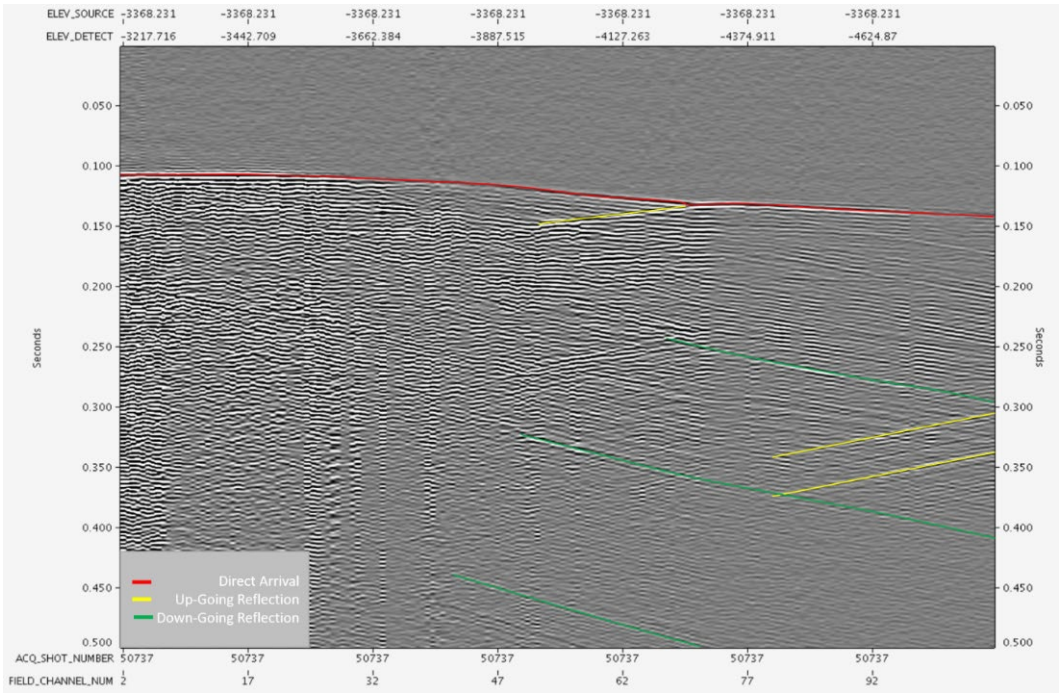

Figure 3-6. Example Compressional Source Gather (TVD -3368.23m)

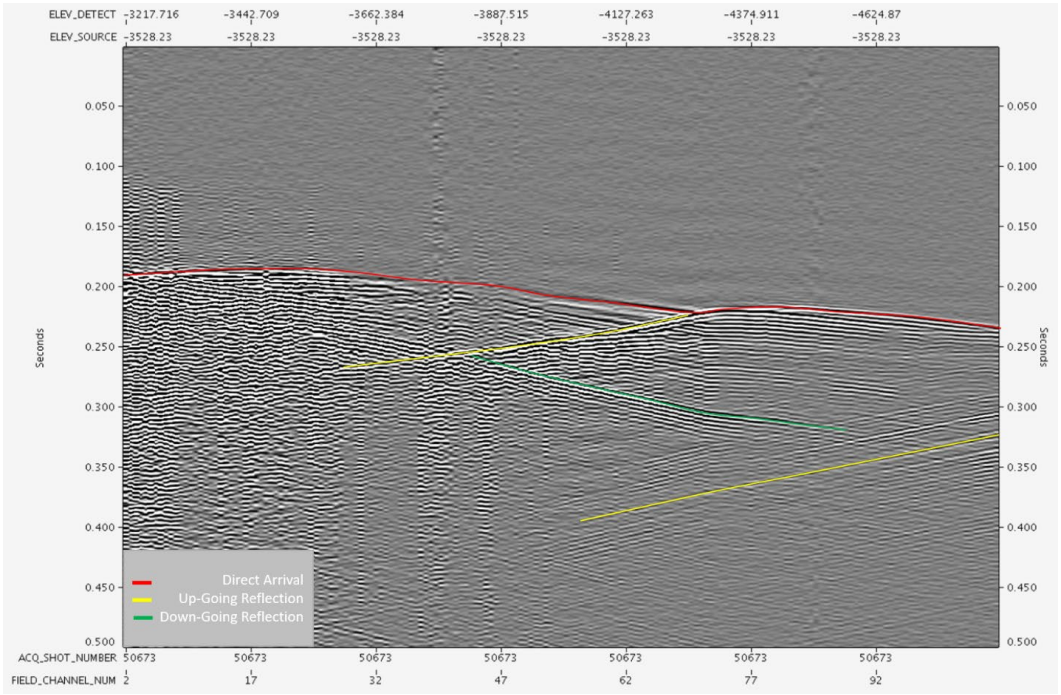

Figure 3-7. Example Shear Source Gather (TVD-3528.23)

3.2 Direct Arrival Picking

Figure 3-8 and Figure 3-9 show example source and receiver gather images with picked direct arrival times.

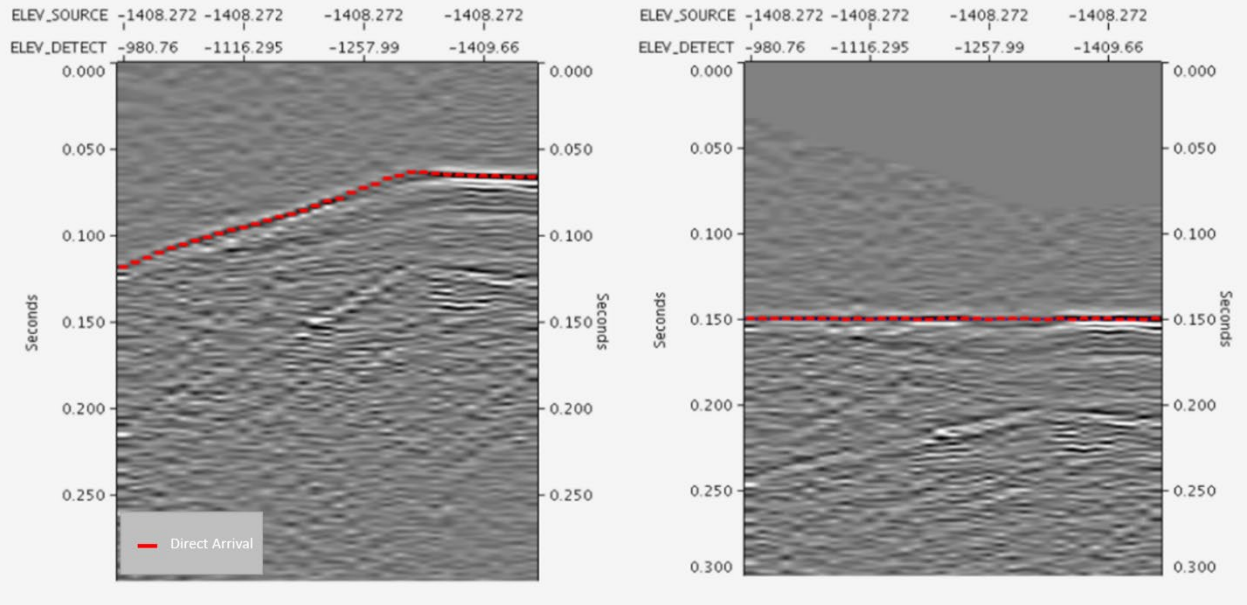

Figure 3-8. Left – Example Compressional Direct Arrival Picking in a Source Gather. Right – Travel Time Shift

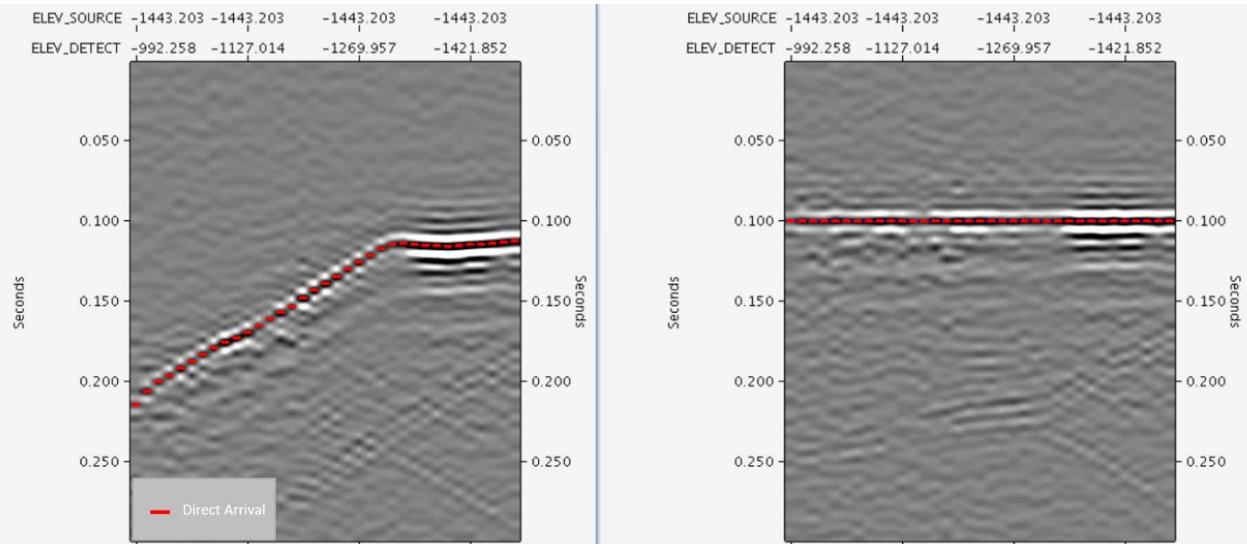

Figure 3-9. Left – Example Shear Picking Source Gather. Right – Travel Time Shift

3.3 Inversion

Figure 3-10 and Figure 3-11 illustrate the inversion process for calculating p- and s-wave velocities and in the process reducing p- and s-wave tomography residuals (i.e., the difference between ray trace travel time and actual measured travel times). Figure 3-12 and Figure 3-13 show the resulting final p and s tomograms.

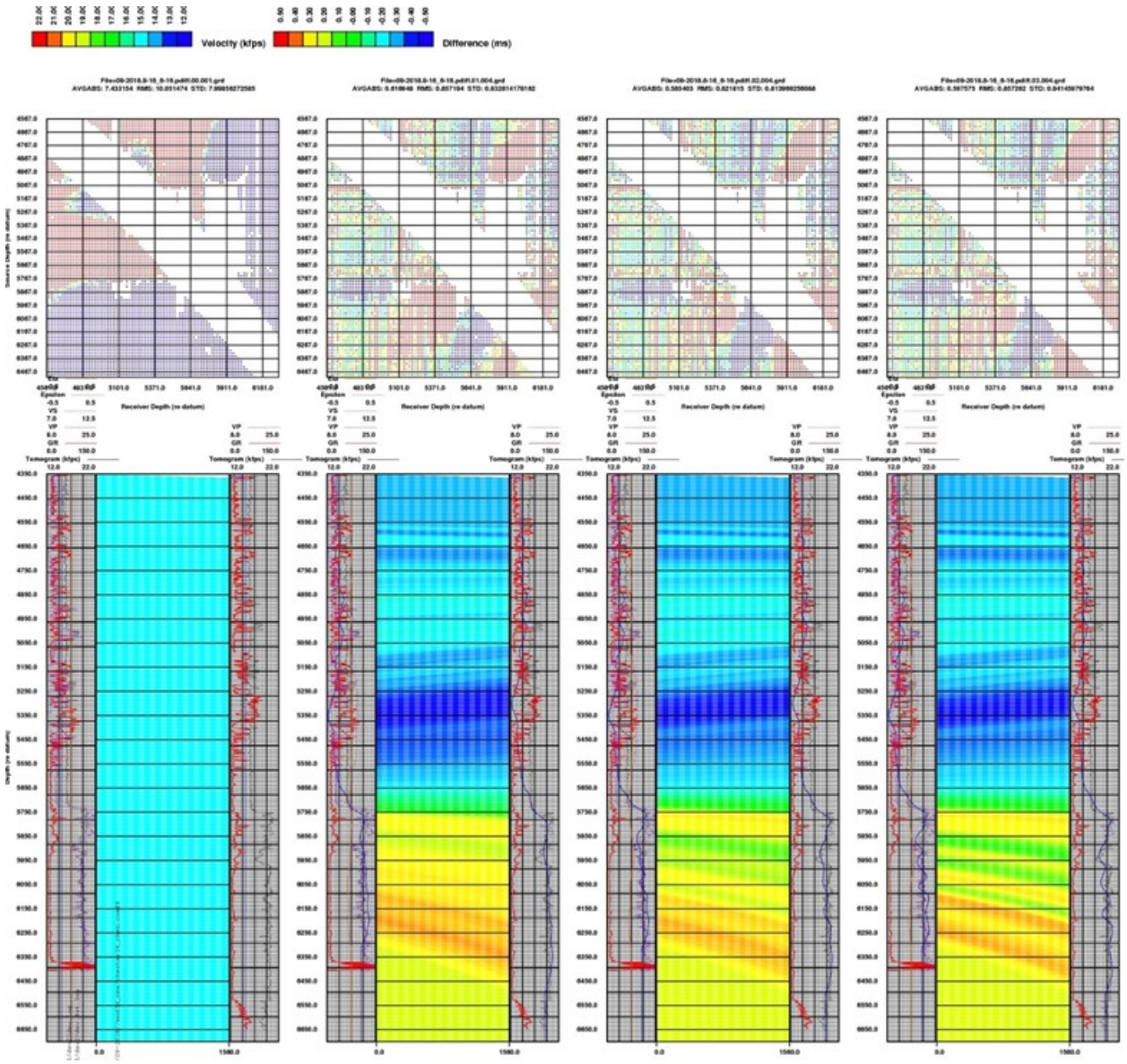

Figure 3-10. The inversion progression begins with a constant velocity model and solves for higher spatial frequencies each continuation step. This figure illustrates the inversion progression. The left-most panel shows the constant velocity model (cyan ~15,000 ft/s) along with the difference times in the grid above. Each panel to the right solves for a higher spatial frequency, increasing the resolution of the tomography and decreasing the difference grid.

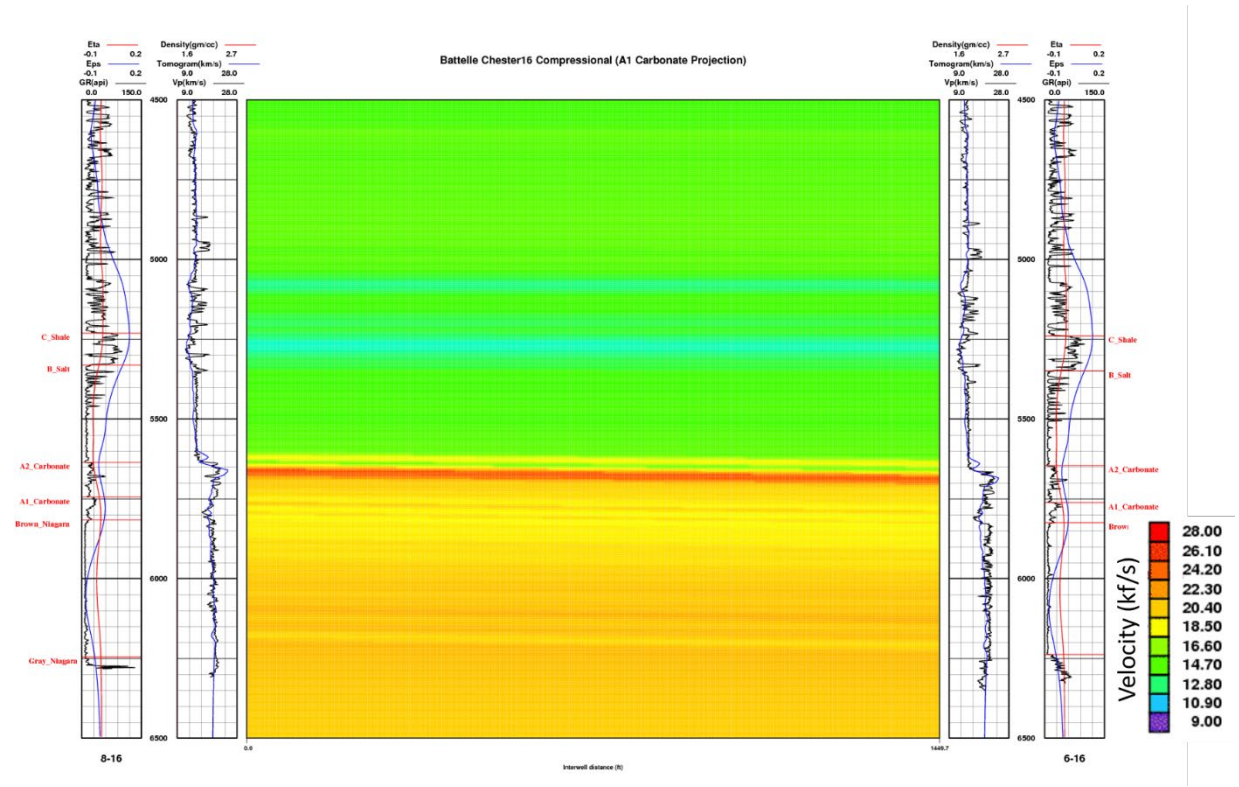

Figure 3-11. Final Compressional Tomogram showing agreement to sonic log at wells

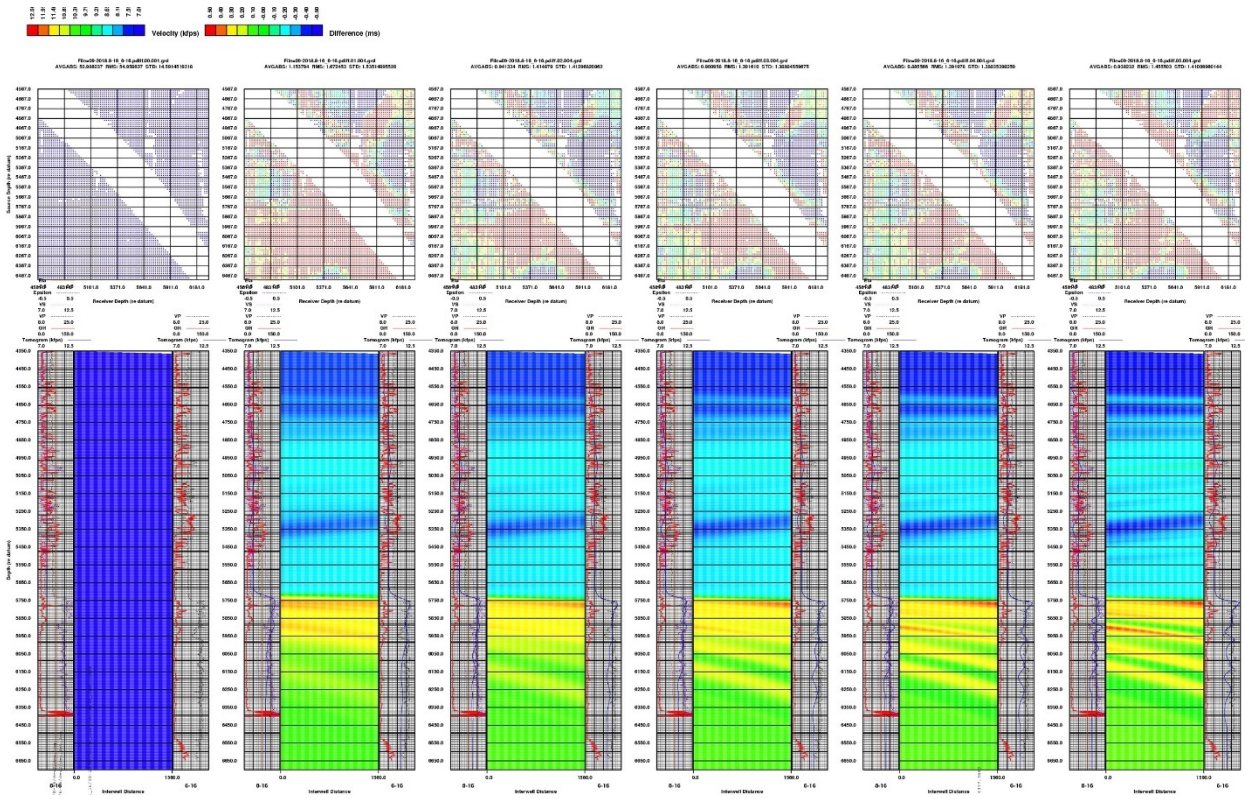

Figure 3-12. Shear Tomography Progression Panel.

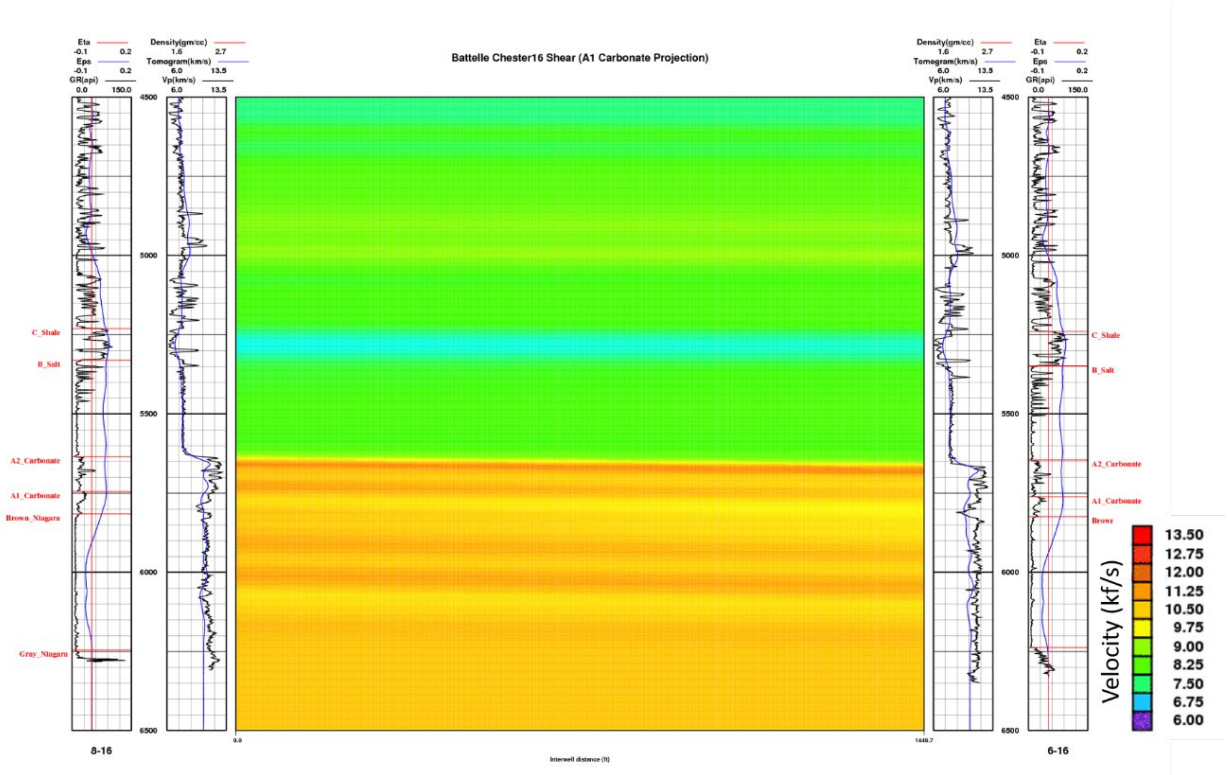

Figure 3-13. Example Final Shear Tomogram

3.4 Low Frequency Correction

To correct for the attenuation of the low frequencies seen in the data, a spectral tilt filter was used to increase the amplitude of those frequencies. This is accomplished by multiplying the Fourier coefficients of those lower frequencies to raise their amplitude. Figure 3-14 and Figure 3-15 show examples of the corrected p-wave and s-wave frequency spectra, respectively.

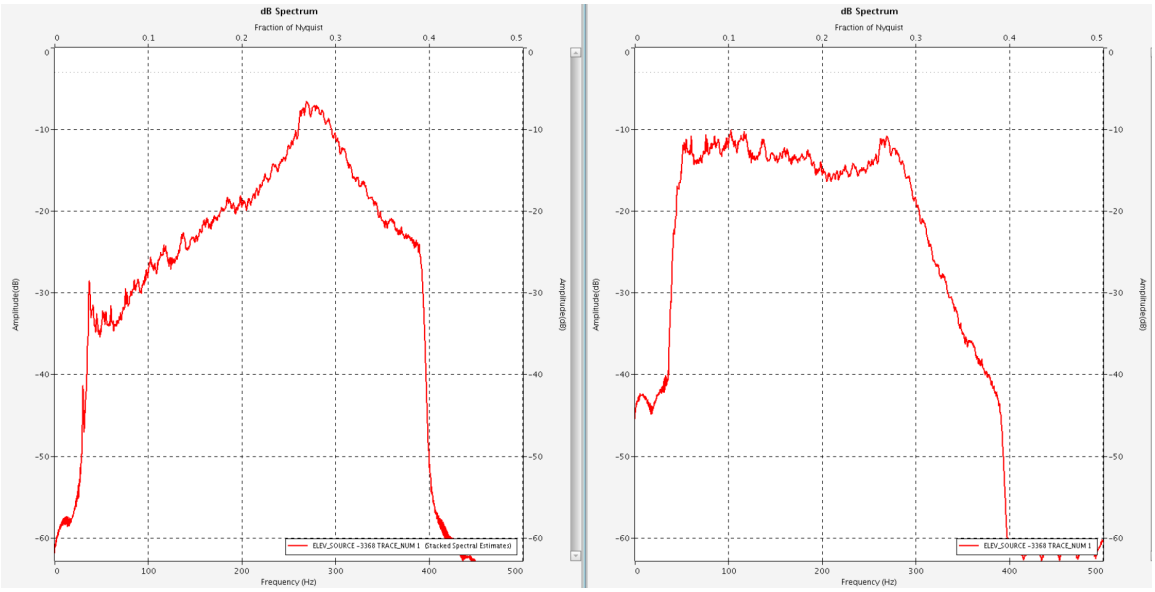

Figure 3-14. Example Shear Frequency Correction Spectrum

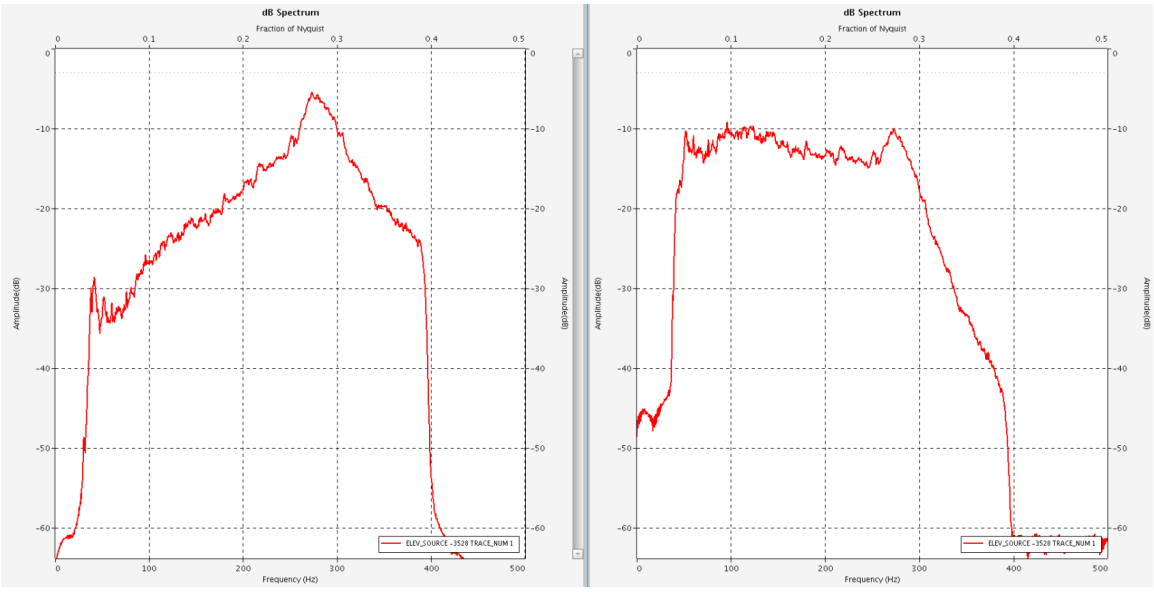

Figure 3-15. Example Shear Frequency Correction Spectrum

3.5 Anomalous Amplitude Attenuation (AAA); Wavefield separation

AAA removes spurious amplitudes from the data, including ringing associated with bad coupling. Wavefield separation, to separate the up-going from the down-going reflections, was done using a τ-p algorithm. Due to the complex nature of the wavefield in some areas, a light touch was used during filter, as not to remove desired reflections. Figure 3-16 and Figure 3-17 show an example p- and s-wave source gather before and after the τ-p algorithm.

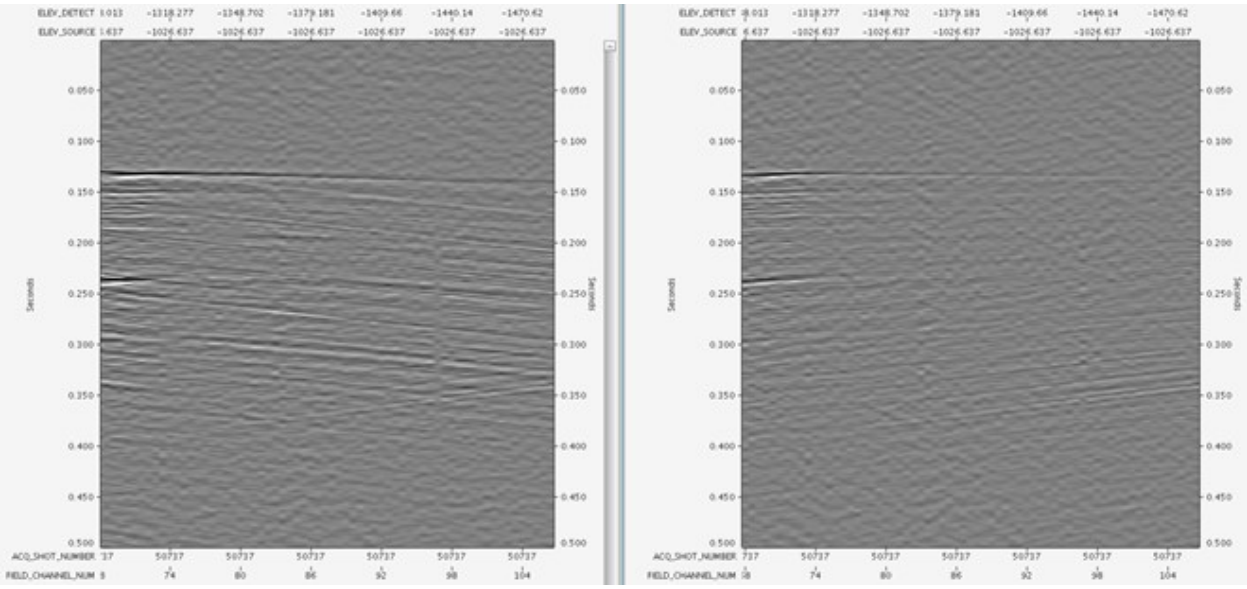

Figure 3-16. Example Compressional Wavefield Separation Source Gather

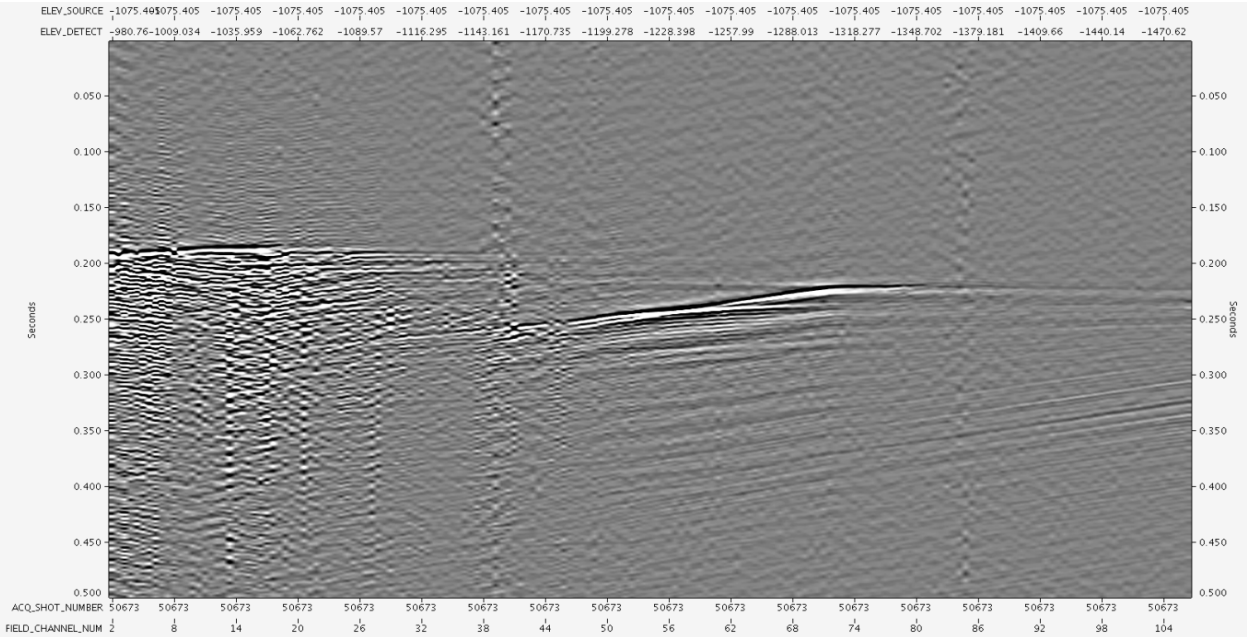

Figure 3-17. Example Shear Wavefield Separation Source Gather

3.6 Angle vs Amplitude (AVA) Volume; Stacking

While the velocity tomogram matched well with the velocity logs, the AVA gather did not fare as well. Ideally, each of the gathers in an AVA volume would be flat, indicating that regardless of the inclination angle, the reflector is being imaged at the same depth. The example p-wave and s-wave AVA gathers are shown in Figure 3-18 and Figure 3-19. These figures show indications of flat layers, but there are significant imaging artifacts due to unwanted wave propagation modes within the data and a polynomial basis that does not accurately describe the reef structure.

The stacking incident angle range of 45-60° was chosen and is shown in Figure 3-20 and Figure 3-21 (which are composite tomogram and reflection images) for compressional and shear data, respectively, with the receiver on the left and the source on the right. A significant limitation of the standard cross-well imaging workflow is reducing the image to a single projection plane. For profiles that can be described by a single projection plane, the solution works well, but the result does not perform as well with highly deviated wells seen in Figure 3-20 and Figure 3-21.

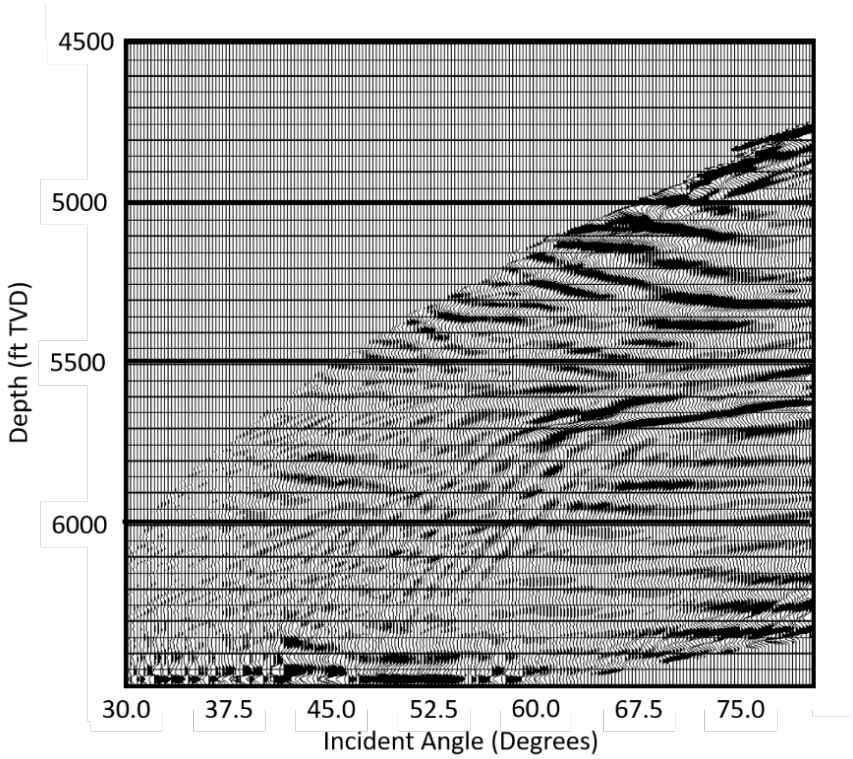

Figure 3-18. Example Compressional Data AVA Gather, Offset 815 ft from the Receiver.

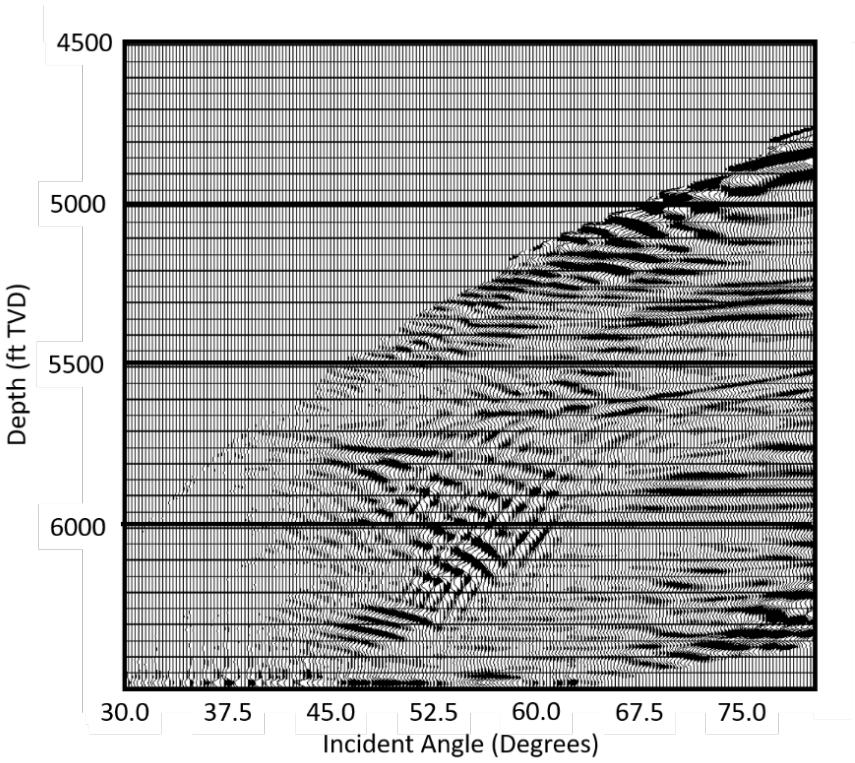

Figure 3-19. Example Shear Data AVA Gather, Offset 815 ft from the Receiver.

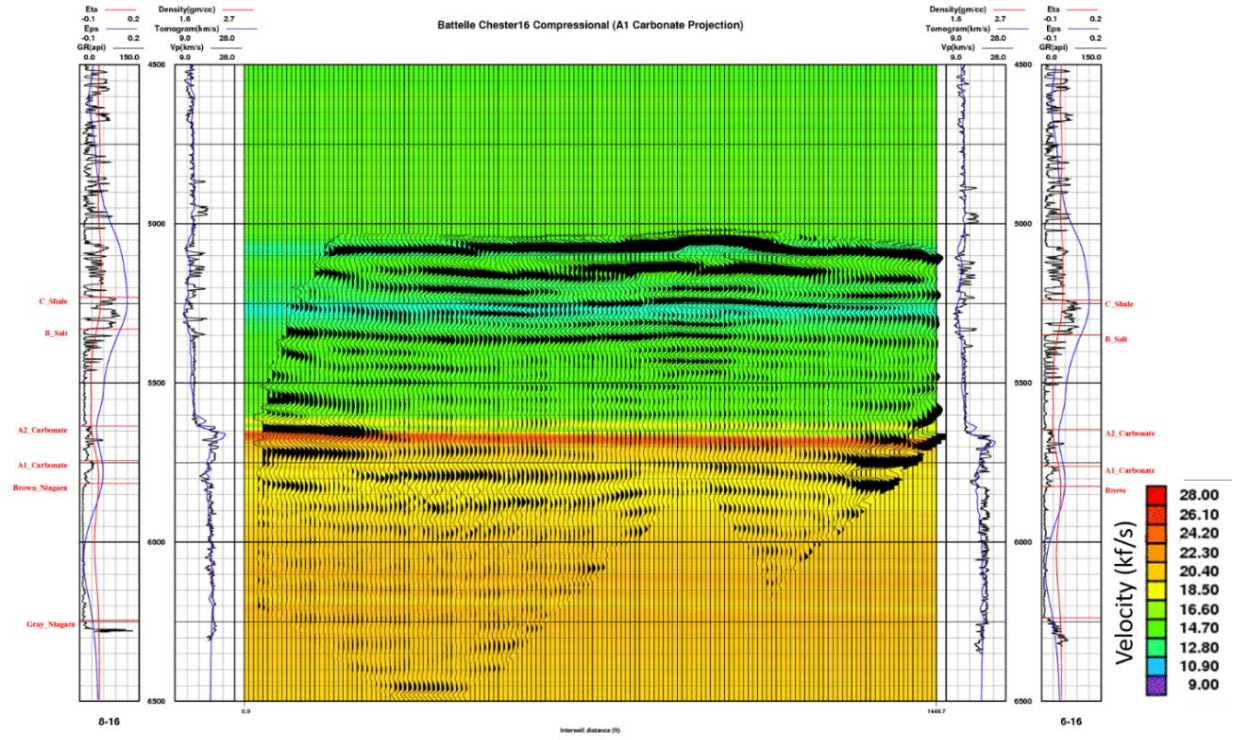

Figure 3-20. Example Compressional Composite (Tomogram and Reflection) Image.

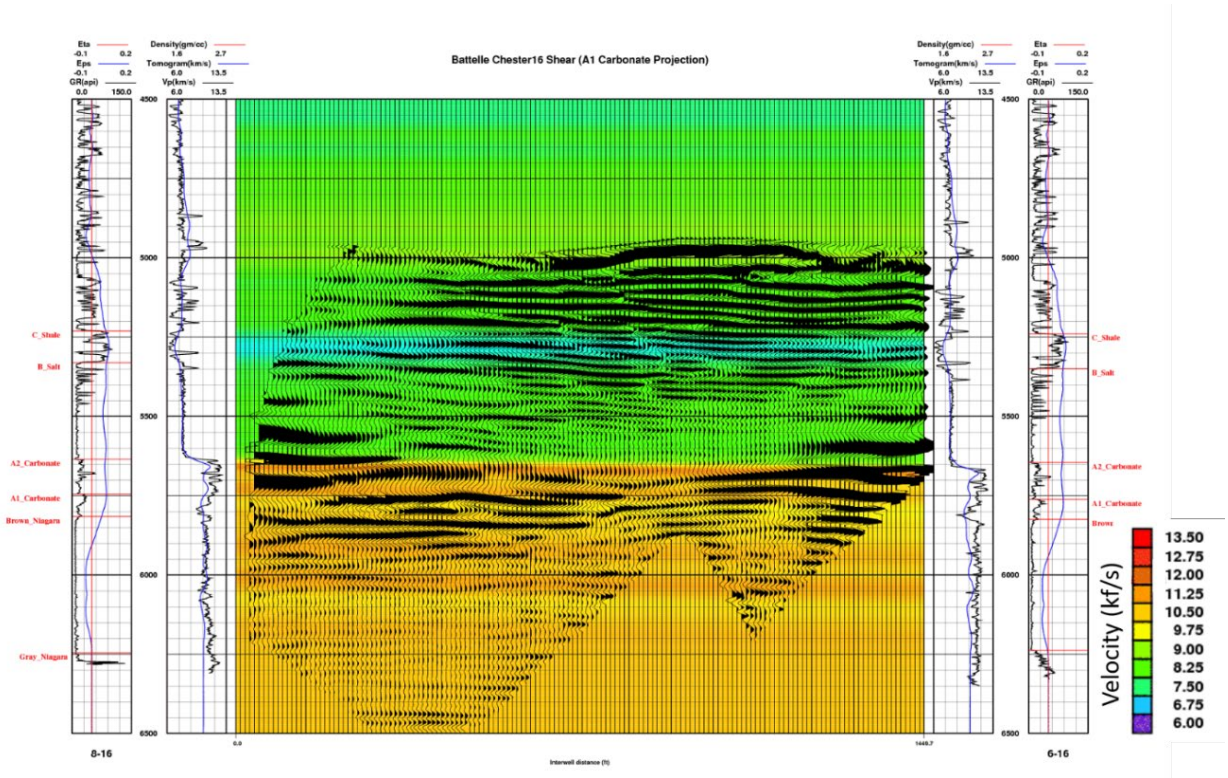

Figure 3-21. Example Shear Composite (Tomogram and Reflection) Image.

4.0 Full Waveform Inversion (FWI)

FWI is non-linear data-fitting procedure that obtains detailed estimates of subsurface properties (i.e., velocities) from seismic data, which can be the result of either passive or active seismic experiments (University of British Columbia, Seismic Laboratory for Imaging and Modeling, 2020). Given an initial guess of the subsurface parameters (a model), the data are predicted by solving a wave-equation. The model is then updated in order to reduce the misfit between the observed and predicted data. This is repeated in an iterative fashion until the data-misfit is sufficiently small. A schematic overview is given in Figure 4-1.

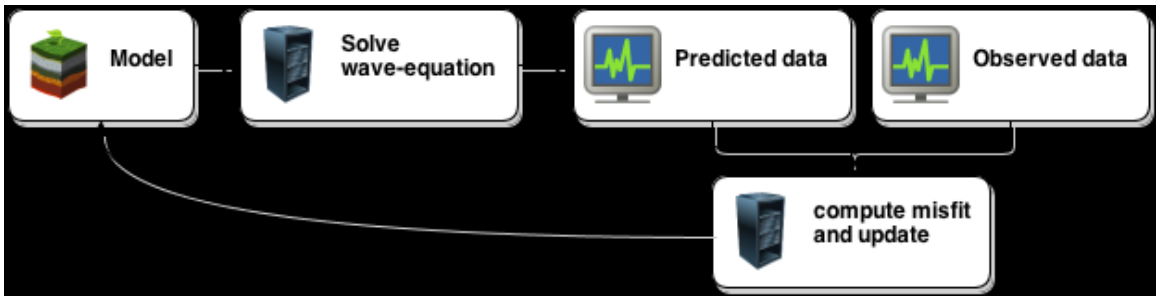

Figure 4-1. Schematic overview of the full waveform inversion workflow
(source: University of British Columbia, Seismic Laboratory for Imaging and Modeling (2020))

In preparation of doing FWI, a 3D static earth model was built using the Schlumberger earth modeling software Petrel with the receiver and source locations populated along with the point sets of the A-2 Carbonate, A-2 Evaporate and Brown Niagaran horizons. Using these horizons, a gross structure of the project area was created, shown in Figure 4-2.

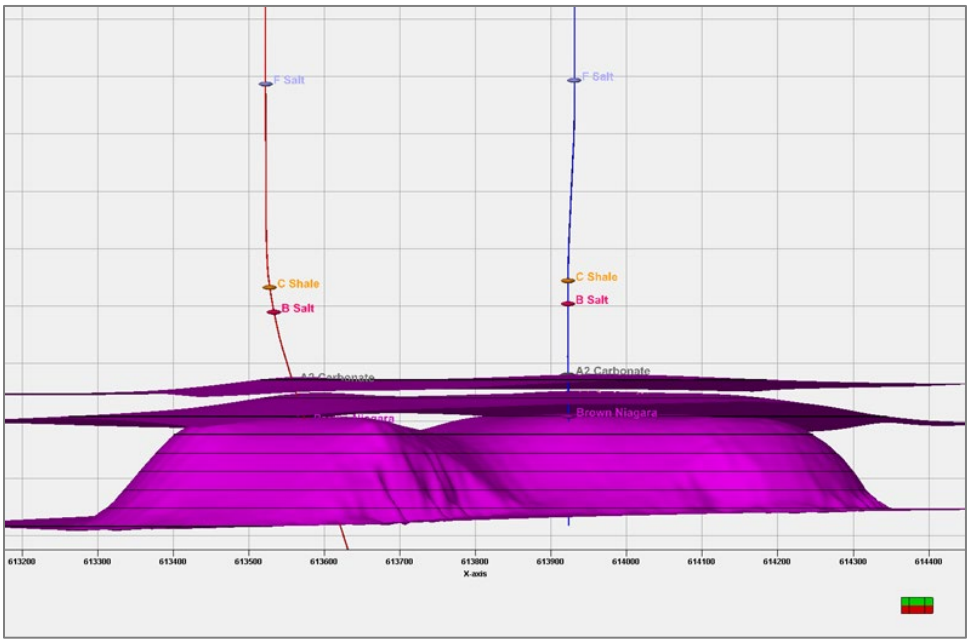

Figure 4-2. Surfaces for Brown Niagaran, A-2 Evaporite, and A-2 Carbonate

4.1 FWI Workflow

Figure 4-3 shows the general workflow for the Schlumberger FWI procedure. The FWI process requires an initial (velocity) model. In a typical time-lapse study, the initial velocity model would be created from the baseline (pre-CO_2 injection) cross-well seismic survey. However, in this study, a baseline cross-well seismic survey was not conducted. Therefore, an attempt was made to use the generated cross-well (polynomial) compressional tomogram (Figure 3-10) as the baseline model; however, the FWI algorithm did not update (revise) this initial velocity model significantly when attempting to solve the post-injection velocity distribution. Therefore, an alternate initial velocity model was created using pre-injection well (sonic) logs, realistic formation surfaces, and anisotropy estimates from the cross-well tomogram (Figure 4-4). This initial velocity model represents the pre- CO_2 injection baseline velocity field. Then, a post- CO_2 injection velocity distribution is calculated using a wavelet (Figure 4-5) extracted from the actual cross-well seismic data. Figure 4-6 shows the final post-CO_2 injection velocity distribution using a wavelet with a frequency of 55 Hz. The process is repeated using gradually higher frequency wavelet (in this study, the process was successfully done with 55 Hz and 75 Hz wavelets. However, the algorithm did not work with higher frequencies even though source frequencies up to 400 Hz were acquired). Then, the pre/post injection models are differenced to arrive at the final image in the workflow, which shows change in velocity due to CO_2 injection.

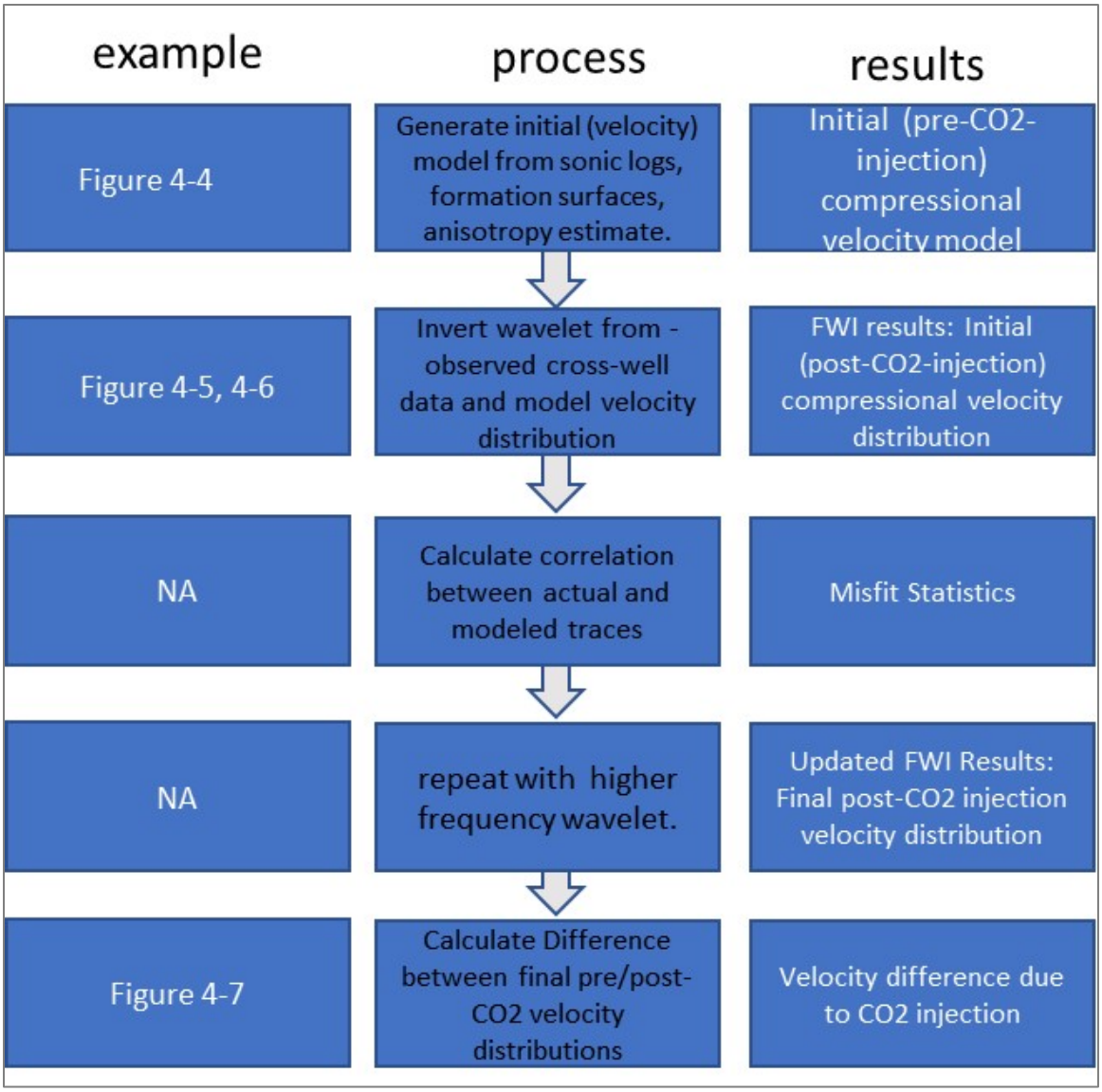

Figure 4-3. FWI Workflow used in this study.

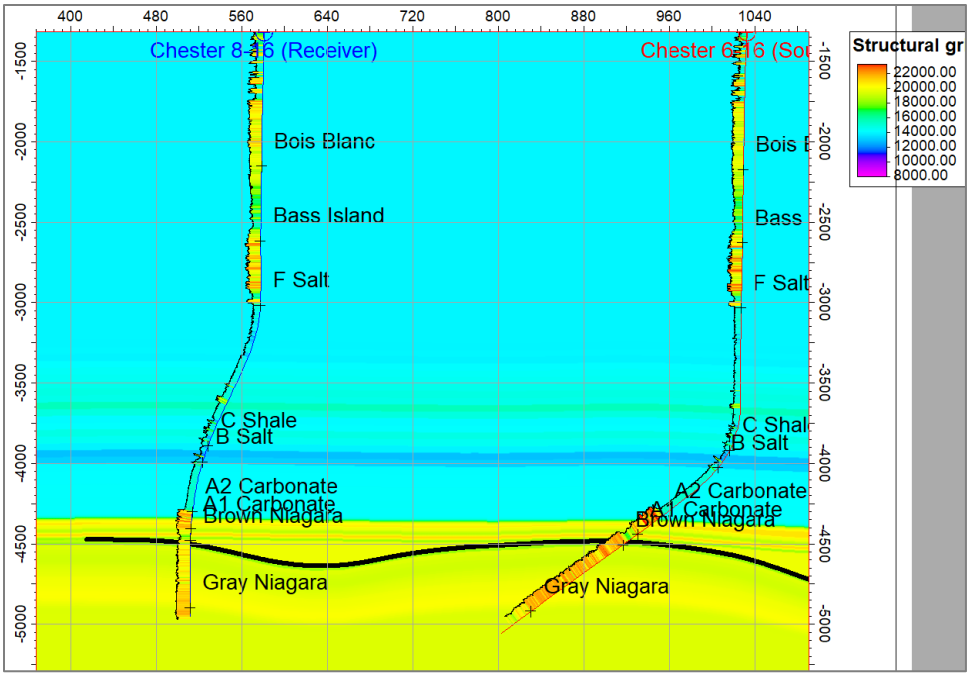

Figure 4-4. Compressional Well Log Initial (Velocity) Model represents initial estimate of Post-CO_2 velocity distribution. Bold line is top of Brown Niagaran. Velocity contrast (blue-yellow contact) occurs at the top of the A-2 Carbonate/base of B-2 Salt.

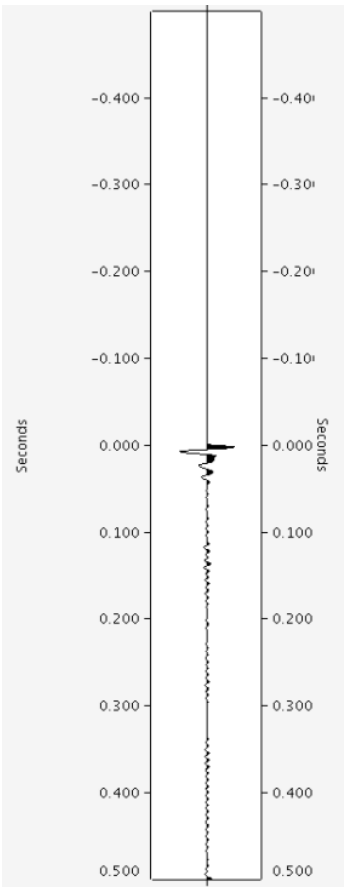

Figure 4-5. 55 Hz Wavelet extracted from actual cross-well seismic data.

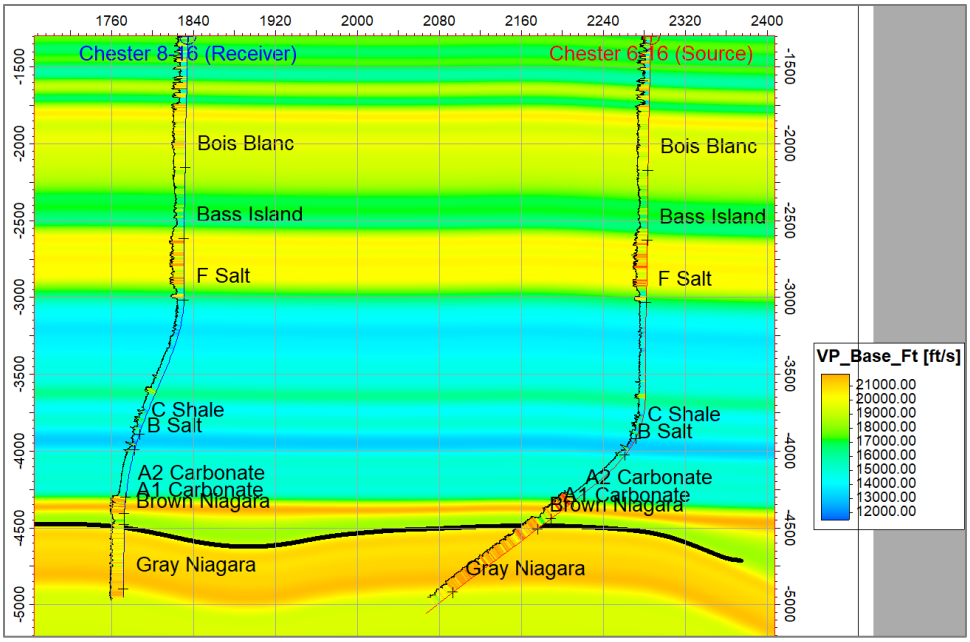

Figure 4-6. Compressional FWI 55Hz Update Model.

4.2 FWI results

The images presented in Figure 4-7 and Figure 4-9 show the interpreted CO_2 distribution (i.e., plume) based on the cross-well waveform tomography results. Figure 4-7 is the result of the FWI algorithm at 55Hz subtracted from the starting model, created from the sonic logs and the anisotropy from the cross-well polynomial-based inversion to arrive at a difference tomogram. The most obvious feature in this figure is the collection of small discontinuous areas of apparent velocity change, with magnitude spanning from -400 (blue) to +600 ms (red), arranged in a swirl pattern around the two wells. These features are interpreted to be artifacts of the finite difference wavefield modeling. This is supported by the fact that these swirls are also present in the RTM imaging results, which is shown in Figure 4-8. As is the case with the FWI method, the RTM algorithm also uses a finite difference process that propagates a wave. While the swirls appear to be anomalous, there is at least one zone that is plausibly due to the CO_2 plume, specifically the large purple-colored lens-shaped area just above the Brown Niagaran near the 8-16 monitoring well where velocity decreased by 600 ms. The location of this “cold spot” coincides with the A-1 Carbonate, which is one of two zones where CO_2 was injected at the 6-16 well. Also, this result is corroborated by other monitoring results (Distributed Temperature Sensing [DTS], PNC, pressure monitoring) for the Chester 16 reef. This also indicates the existence of the CO_2 plume in this same interval at the monitoring well location. The purple cold spot extends laterally in the A-1 Carbonate toward the injection where a blue cold spot (-400 ms) occurs. The two zones do not connect, but this may be the result of projecting the results onto a single 2D plane. (Note however that the two purple zones do connect in Figure 4-9.)

- Both cold spots (areas of velocity decrease) and hot spots (areas of velocity increase) are present in Figure 4-7. A small velocity decrease is consistent with CO_2 displacing methane. This is the expected situation for the Chester 16 reef that was initially pressure depleted when CO_2 injection began (owing to primary production that reduces reservoir pressure) with high levels of methane present (due to methane exsolving from the liquid as reservoir pressure is decreased). As CO_2 is injected, the reservoir pressure increases, which drives the methane back into solution such that the CO_2 becomes the main pore-occupying fluid. This scenario was analyzed using rock physics (fluid substitution) modeling for the Dover 33 reef which estimated a velocity decrease on the order of 1% for the A-1 Carbonate/Brown Niagaran (see companion monitoring report on the Dover 33 VSP monitoring study). Initial velocity for the A-1 Carbonate, as shown in Figure 4-4, is on the order of 20,000 ms; therefore, the velocity decrease predicted by the FWI process (-600 ms) is a change of approximately 3%, slightly greater than the estimate of a 1% decrease but still highly similar.
- Figure 4-7 and Figure 4-9 display swirls of “hot” (velocity increase) and “cold” (velocity decrease) spots around the two wells; however, the cold spot (velocity decrease) in the A-1 Carbonate is plausible, as demonstrated with DTS monitoring, pressure monitoring, and PNC-log monitoring, all of which point to the A-1 Carbonate as the primary conduit for CO_2 injected at the 6-16 well.
- The hot spots in Figure 4-7 (yellow, red) are suspect. Fluid substitution involving CO_2 replacing methane, brine or oil would all likely result in a velocity decrease, not a velocity increase. Similarly, it is well- known that an increase in effective pressure (decrease in pore pressure) can cause an increase in velocity; however, an increase in pore pressure (decrease in effective pressure) will result in a decrease in velocity. Therefore, the hot spots (red, yellow) in Figure 4-7 are likely to be anomalies.
- The cold spots in the layers above the A-1 carbonate are also suspect. These layers include the A-2 carbonate, B-salt, C-Shale, and F-Salt, all which have very low permeability and thus would not likely transmit CO_2.
- Many of the hot/cold spots have a very small magnitude, representing a very small change, as low as 150 to 200 ft/sec. For example, above the Bass Island horizon there are a lot of green and cyan swirls

indicating a very small velocity difference of approximately 150 or 200 ft/s. These velocity changes are likely close to the detection limit of the cross-well seismic technology.

- Noise in the data may be affecting the FWI update. Both high velocity differences at the Gray Niagara are very suspicious because they occur right at the wellbore. This means that the velocity error calculated (real – modeled data) was very close to, or at/on, the direct arrival. (Note: If the velocity model and RTM imaging are correct, the direct arrival will image along the wellbore.) To have a high amplitude at the wellbore means the true data direct arrival was significantly different than the modeled data, at the direct arrival, but only there.

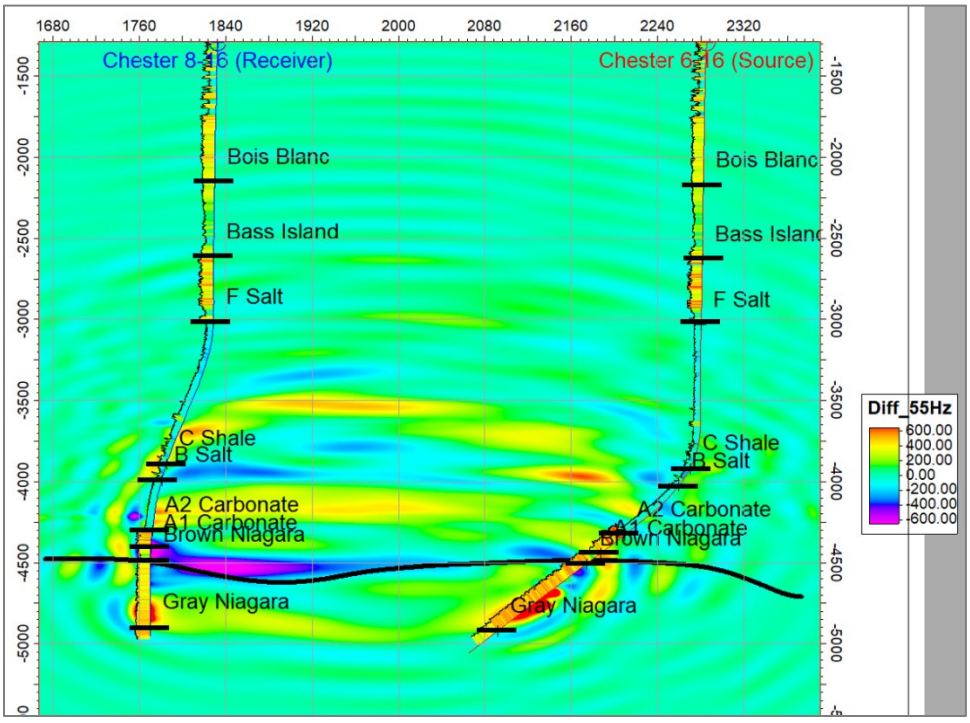

Figure 4-7. Compressional Velocity Difference Tomogram for 55 Hz Source Wavelet. Bold line is top of Brown Niagaran. Zone of major velocity change occurs in A-1 Carbonate.

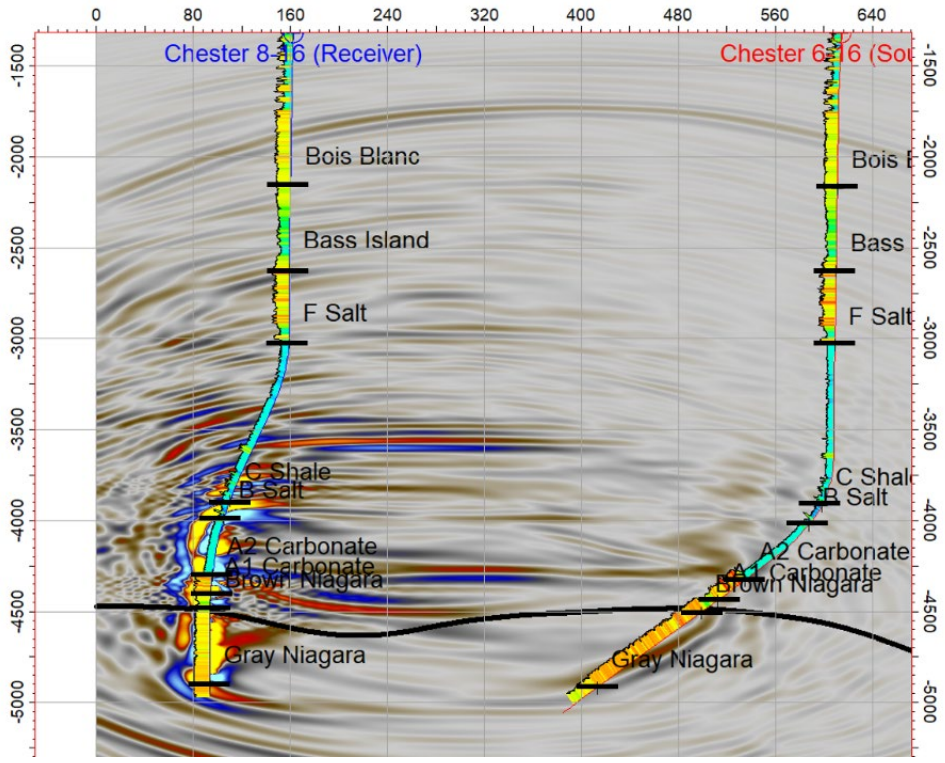

Figure 4-8. Compressional RTM Reflection Image showing swirl pattern

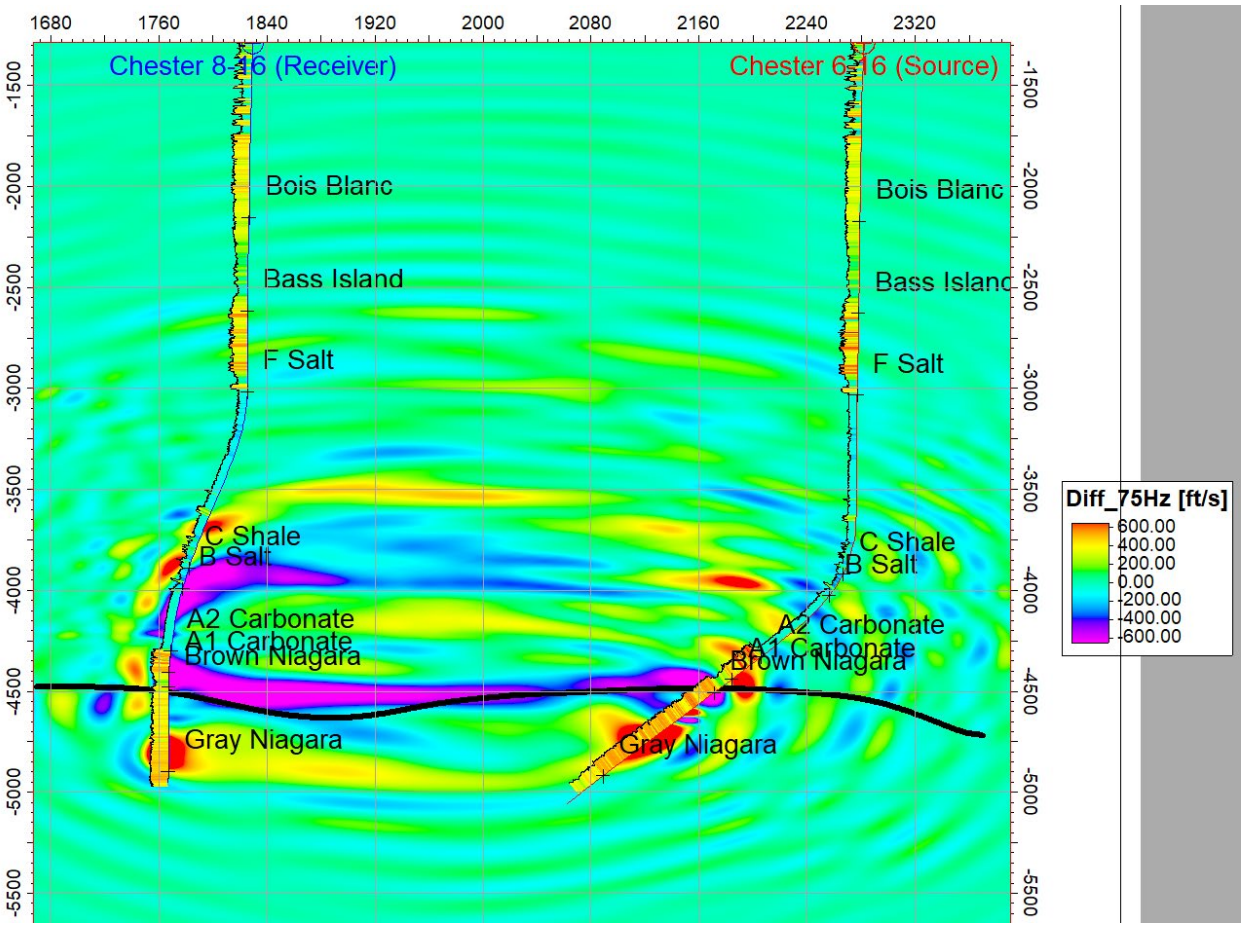

Figure 4-9. Compressional Velocity Difference Tomogram for 75 Hz Source Wavelet.

5.0 Summary

Cross-well seismic is always a complex technology. In this study, it was made more challenging by several causes. Implementing it in deviated wells and complex geology are two examples of challenges associated with this study. These and other factors are mentioned below.

Acquisition Geometry – The acquisition geometry affected two key aspects of the project, including the frequency spectrum and the component rotations and the resulting datasets.

- **Frequency Spectrum** – The inclination of the source well directly affected the frequency spectrum of the data. The Z-Trac is a mechanical shaker source with a heavy tungsten source. At low starting frequencies (30-250 Hz), the mass is difficult to accelerate and create significant amplitudes in the recorded traces. Figure 5-1 shows a spectrum of an example trace from the shear data before and after amplitude correction using a spectral tilt filter
- **Component Rotations** – The component rotations were generally excellent, but there were some areas within the data volume that had higher error in the rotation calculation. Frequently, the greatest error in the component rotation was seen in the zone most likely to be affected by the CO_2 plume. This is an expected result if those traces passed through the plume. The higher error of the component rotation affects the wavefield separation and the imaging. Errors in the rotation angle can leave shear waves amplitudes in the compressional data and vice versa. When imaging, the traces contaminated with other modes can create artifacts within the image.

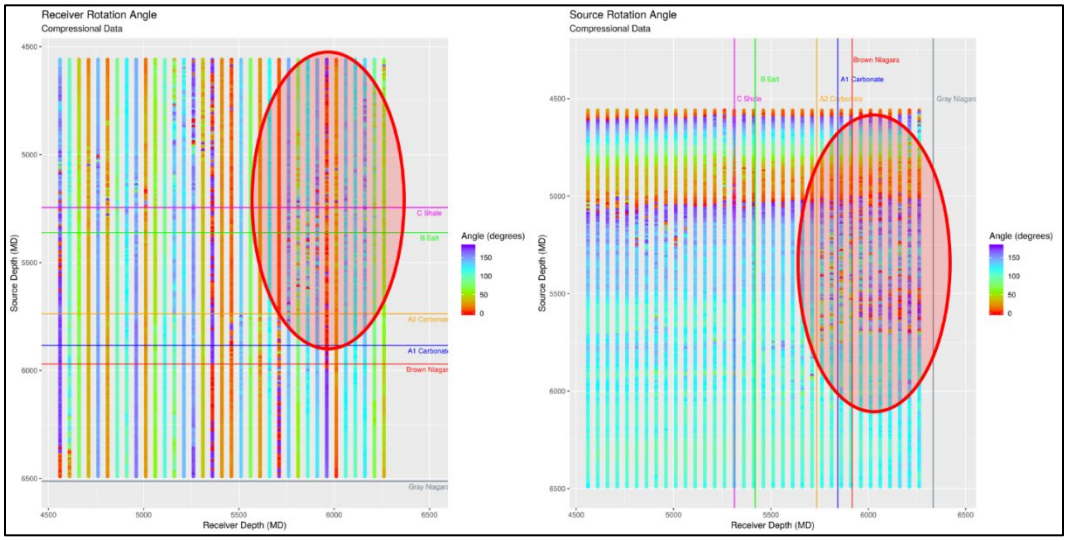

Figure 5-1. Fan 5 Receiver and Source Rotations with Higher Error Identified.

Imaging Plane – The highly deviated wellbores add additional complexity to the imaging process. The standard cross-well imaging workflow requires a single vertical, imaging plane to project the migrated and stack image. Typically, a best-fit line between the wellbores is calculated and is used as the imaging plane. For this project, there is no single plane that accurately captures the effects of the depth-varying trajectories of the wells; therefore, a lane near/through the A-1 Carbonate was selected because this is believed to be the primary conduit for lateral CO_2 migration away from the injection well.

Complex Geology – The reef contains two structural features that complicate processing and interpretation of the cross-well data; these include a saddle near the center of the cross-well profile, and steeply sloping contacts between layers normal to (i.e., at each end of) the profile. These features

combined with the depth varying trajectory of both wells precluded the use of the standard Schlumberger cross-well processing/interpretation workflow.

Full Waveform Inversion – While it is believed that FWI was successfully implemented in this study to delineate CO_2, the results were adversely effected by the following issues:

- Starting Model – The starting model for the FWI algorithm was a mix of the compressional velocity log and the anisotropy values found using the cross-well tomography. An attempt was made to use the compressional velocity data from the cross-well tomography converted using the anisotropy ellipse (Figure 5-2) to convert the angled velocity calculation to a vertical velocity calculation. The resulting FWI velocity update showed little to no change after inversion, whereas using the compressional log did show a significant change. There are numerous reasons why the vertical velocity worked better than a projected vertical velocity. More than likely, the anisotropy estimates include error that propagates into the vertically projected velocity.

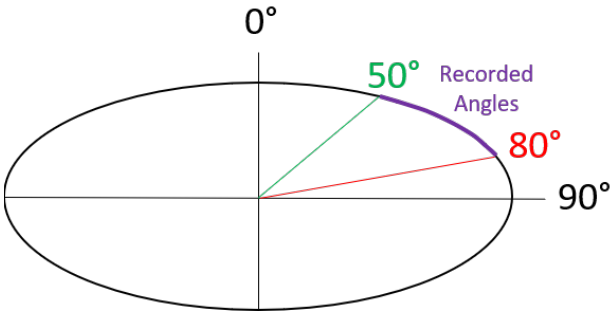

Figure 5-2. Anisotropy Ellipse with Recorded Cross-well Seismic Angles.

- Maximum Source Frequency – The Schlumberger FWI algorithm has a maximum frequency limit of approximately 75Hz. Attempts of inversion runs at both 85 and 100Hz were made and failed. Thus, it was not possible to utilize the full frequency range of the source (400 Hz). The algorithm was originally intended for surface seismic and is adequate for that application.
- Shear-Wave Data – Schlumberger has not developed a FWI algorithm for shear-wave data; thus, it was not possible to use the different response of P and S waves to help delineate CO_2. Without the shear-wave data, p-wave data alone had be used to delineate the CO_2. Fortunately, the FWI method doesn't require a baseline survey.

6.0 Conclusions

Time-lapse cross-well seismic has been used elsewhere to monitor CO_2 injected into the subsurface, see Table 6-1 for two well-known examples. In these examples and all other cross-well studies found in the literature, a pre-injection baseline study was performed. However, in this study, a baseline cross-well survey was not obtained; nevertheless, it was still possible to generate an image that is a plausible representation of the CO_2 plume. This conclusion is supported by other monitoring and modeling results from the Chester 16 reef that provide an independent indication about the likely position of the injected CO_2. To the authors' knowledge, this is the first time this has been done. There no precedents for a successful cross-well seismic survey without a baseline survey, nor are there known examples of cross-well seismic examples in carbonate pinnacle reefs or using deviated wells.

Table 6-1. Selected Examples of Previous Crosswell Seismic Studies.

	Source	Primary method
Cranfield large-scale CO_2 injection pilot	Ajo-Franklin, J.B. , Peterson, J, Doetsch, J, Daley, T.M., 2013.	Time-lapse tomography difference results integrated with secondary datasets including RST, SP, and sonic identified (visibly) two laterally continuous zones of significantly decreased P-wave velocity due to CO_2 invasion. CO_2 zones correspond to higher permeability sections of the reservoir.
Ketzin Germany field CO_2 injection pilot	Zhang, Fengjiao, Juhlin, Christopher, Cosma, Calin Tryggvason, Ari and R. Gerhard Pratt, 2012.	Travel-time tomography images of the real data show no observable differences between the surveys. However, seismic waveform tomography difference images show significant differences. A number of these differences are artefacts that can probably be attributed to inconsistent receiver coupling between the different surveys. However, near the injection horizon, below the caprock, a velocity decrease is present that is consistent with that expected from the injection process. 51,231 tons of CO_2 were injected into a saline sandstone/siltstone reservoir. Up to 21 percent *P*-wave velocity reduction may occur as CO_2 replaces saline water in saturated reservoir sandstone.

7.0 References

Ajo-Franklin, J.B. ,Peterson, J, Doetsch, J, Daley, T.M., 2013. High-resolution characterization of a CO_2 plume using crosswell seismic tomography: Cranfield, MS, USA; International Journal of Greenhouse Gas Control Volume 18, October 2013, Pages 497-509

Harris, J. and R. T. Langan (2001): Crosswell Seismic Profiling: Principle to Application; AAPG Search and Discovery Article #40030 (2001).

University of British Columbia, Seismic Laboratory for Imaging and Modeling (2020). Full waveform inversion (FWI); https://www.slim.eos.ubc.ca/research/inversion; site accessed January 9, 2020.

Zhang, Fengjiao, Juhlin, Christopher, Cosma, Calin Tryggvason, Ari and R. Gerhard Pratt, 2012. Cross-well seismic waveform tomography for monitoring CO_2 injection: a case study from the Ketzin Site, Germany; Geophys. J. Int. (2012) 189, 629–646 doi: 10.1111/j.1365-246X.2012.05375

BATTELLE

It can be done